Behavioural phenotypes and thalamic reticular nucleus impairment in three mouse models of autism spectrum disorder and the effects of a novel MT2 selective partial agonist: a preliminary study

Athanasios Markopoulos, B.Sc.

Integrated Program in Neuroscience

Neurobiological Psychiatry Unit, Department of Psychiatry, McGill University, Montreal

September, 2022

A thesis submitted to McGill University in partial fulfillment of the requirements of the degree of Master of Science

TABLE OF CONTENTS

ABSTRACT

Autism spectrum disorder (ASD) is a prevalent neurodevelopmental disorder characterized by reduced social behaviour and communication. To date, there is a lack of effective pharmacological treatment options that target the characteristic dysfunction in social behaviour for individuals with ASD. This disorder can be caused by many genetic, epigenetic, and environmental factors, and the characterization of genetic syndromes associated with ASD has given rise to transgenic mouse models of ASD that recapitulate many of the behavioural and neurobiological phenotypes observed in humans. Examples of these are Fragile X syndrome, Tuberous Sclerosis Complex, and Phelan McDermid syndrome, which arise from mutations to the Fragile X Mental Retardation Protein 1 (*Fmr1*), Tuberous Sclerosis Complex 2 (*Tsc2*), and SH3 and multiple ankyrin repeat domains 3 (*Shank3*) genes, respectively. The present study sought to characterize the behavioural phenotypes of mice with mutations to these genes: the *Fmr1* hemizygous KO, *Tsc2* heterozygous KO, and *Shank3* homozygous KO mouse lines, for which we hypothesized that all would display reduced social behaviour as a main outcome. We found that of the three mouse lines, only *Fmr1* KO mice exhibit reduced social behaviour. They also demonstrated a trend for reduced anxiety-like behaviour. No differences were found between the *Tsc2 WT* and KO mice, while *Shank3* KO mice were found to be hyperactive. Furthermore, in these mice, we sought to characterize the electrophysiological activity of the thalamic reticular nucleus, an inhibitory thalamic structure that has been hypothesized to be greatly impacted in the pathogenesis of ASD and is rich in the melatonin type 2 (MT2) receptor. We hypothesized that we would find abnormal firing in the TRN of all three mouse models mice. *In vivo* single unit recordings revealed that *Tsc2* KO mice had reduced TRN firing and burst activity, *Shank3* KO mice had increased TRN firing and burst activity, and *Fmr1* showed a trend of reduced TRN firing. Lastly, we tested the behavioural and

electrophysiological effects of a MT2 partial agonist, UCM924, to see if its administration can reverse any of the behavioural phenotypes and TRN dysfunction in these mouse models. Treatment with UCM924 increased the social behaviour of *Tsc2* mice, while also showing an anxiolytic trend for these mice. Additionally, in the TRN, UCM924 increased the firing and burst activity of *Fmr1* and *Tsc2* KO mice, while decreasing the firing rate of *Shank3* KO mice. In conclusion, only the *Fmr1* KO mice exhibited reduced social behaviour, while a dysfunction in TRN activity was found in the *Tsc2* and *Shank3* KO mice (with a trend in the *Fmr1* KO mice), and UCM924 reversed the altered TRN activity in all three mouse models.

RÉSUMÉ

Les troubles du spectre de l'autisme (TSA) sont un trouble neurodéveloppemental prévalent caractérisé par un réduction du comportement et communication social. À ce jour, il manque d'options de traitement pharmacologique efficaces qui ciblent le dysfonctionnement du comportement social caractéristique chez les personnes atteintes de TSA. Ce trouble peut être causé par de nombreux facteurs génétiques, épigénétiques et environnementaux, et la caractérisation des syndromes génétiques associés aux TSA a donné lieu à des modèles de souris transgéniques de TSA qui récapitulent des phénotypes comportementaux et neurobiologiques observés chez les humains. Le syndrome de l'X fragile, le complexe de la sclérose tubéreuse et le syndrome de Phelan McDermid en sont des exemples. Ces syndromes résultent de mutations des gènes de la protéine 1 de l'arriération mentale du X fragile (*Fmr1*), du complexe de la sclérose tubéreuse 2 (*Tsc2*), et des domaines SH3 et multiples de la répétition de l'ankyrine 3 (Shank3), respectivement. La présente étude visait à caractériser les phénotypes comportementaux de souris présentant des mutations de ces gènes : les souris Fmr1 KO hémizygotes, Tsc2 KO hétérozygotes et Shank3 KO homozygotes, pour lesquels nous avons émis l'hypothèse que tous présenteraient un comportement social réduit comme résultat principal. Nous avons trouvé que de les trois types de souris, seules les souris Fmr1 KO présentent un comportement social réduit. Elles ont également montré une tendance à la réduction du comportement d'anxiété. Aucune différence n'a été constatée entre les souris Tsc2 WT et KO, tandis que les souris Shank3 KO étaient hyperactives. De plus, chez ces souris, nous avons cherché à caractériser l'activité électrophysiologique du noyau réticulaire thalamique (NRT), une structure thalamique inhibitrice qui est supposés d'avoir un impact important dans la pathogenèse des TSA, et est riche en récepteurs de la mélatonine de type 2 (MT2). Nous avons émis l'hypothèse que nous trouverions de l'activité anormal dans le NRT des

trois modèles de souris. Les enregistrements mono-unitaires *in vivo* ont révélé que les souris Tsc2 KO présentaient une réduction de potentiels d'actions et de l'activité en rafale du TRN, que les souris Shank3 KO présentaient une augmentation des potentiels d'actions et de l'activité en rafale du TRN et que Fmr1 montrait une forte tendance à la réduction des potentiels d'actions du TRN. Enfin, nous avons testé les effets comportementaux et électrophysiologiques d'un agoniste partiel du MT2, l'UCM924, pour voir si son administration peut inverser les phénotypes comportementaux et le dysfonctionnement du TRN dans ces modèles de souris. Le traitement avec UCM924 a augmenté le comportement social des souris Tsc2, tout en montrant une tendance anxiolytique pour ces souris. De plus, dans le TRN, l'UCM924 a augmenté les potentiels d'actions et l'activité en rafale des souris Fmr1 et Tsc2 KO, tout en diminuant les potentiels d'actions des souris Shank3 KO. En conclusion, seules les souris Fmr1 KO ont présenté un comportement social réduit, tandis qu'un dysfonctionnement de l'activité TRN a été constaté chez les souris Tsc2 et Shank3 KO (avec une tendance chez les souris Fmr1 KO), et l'UCM924 a inversé l'activité TRN altérée dans les trois modèles de souris.

ACKNOWLEDGEMENTS

I'd first like to thank Michael Pileggi, Minza Haque and Leora Pearl-Dowler for their help with my research, but more importantly, for making my experience as a MSc student enjoyable. Thank you to Jacques Singer, Emily Grant and Anahita Oveisi for the great vibes. Thank you to Justine Enns for helping me learn behavioural assays and helping me learn how to make important considerations when planning scientific experiments when I first joined the lab. Thank you to Dr. Danilo De Gregorio for teaching me how to design, plan, and perform behavioural assays, electrophysiology and microiontophoresis experiments. He also helped me learn how to think like a scientist and how to interpret results. Also, a big thank you to him for his help with my fellowship/grad school applications. Thank you to Dr. Martha Lopez Canul for her help with EEG experiments, perfusions, scientific guidance, and for her good vibes in the lab. Thank you to Dr. Antonio Inserra for helping me learn electrophysiology, for revising some of my fellowship applications and manuscripts, and for his help collecting and analyzing electrophysiology data. Thank you to my professor Dr. Rochford for teaching me how to conduct ethical research and perform proper and ethical statistics. Thank you to my professor Dr. Sylvia Villeneuve for her help with grad school applications and for helping me learn how to effectively deliver scientific presentations and write grant applications. Thank you to my supervisor Dr. Gabriella Gobbi for supervising my MSc research, for helping me design experiments and interpret results, for her help with fellowship/grad school applications, and for her editorial help with manuscripts and this thesis. Thank you to my thesis committee members Dr. Yang Zhou and Dr. Cecilia Flores for their valuable advice and guidance with my project. I'd like to express my deepest gratitude to my IPN mentor Dr. Kenneth Hastings for his invaluable support throughout my MSc degree. I consider myself extremely fortunate to have benefited from his wise words and active help when I was

presented with obstacles. Thank you to my family and friends for their encouragement and support. Last but not least, thank you Marissa Kyres. I am forever grateful for your constant support, great advice, love, and for listening to all my scientific presentations multiple times.

CONTRIBUTION OF AUTHORS

Ethics and funding: Dr. Gabriella Gobbi

Preparation of thesis: Tommy Markopoulos, revisions by Dr. Gabriella Gobbi

Animal colonies: Dr. Nahum Sonenberg and Ms. Annik Lafrance

Behavioural experiments (with and without UCM924):

Study design: Tommy Markopoulos, Dr. Danilo De Gregorio, Dr. Gabriella Gobbi

Data collection: Tommy Markopoulos

Data analysis: Tommy Markopoulos

Electrophysiology experiments:

Study design: Tommy Markopoulos, Dr. Antonio Inserra, Dr. Gabriella Gobbi

Data collection: Tommy Markopoulos, Dr. Antonio Inserra, Michael Pileggi

Data analysis: Tommy Markopoulos, Dr. Antonio Inserra, Michael Pileggi

Microiontophoresis experiments:

Study design: Tommy Markopoulos, Dr. Danilo De Gregorio, Dr. Gabriella Gobbi

Data collection: Tommy Markopoulos, Dr. Antonio Inserra

Data analysis: Tommy Markopoulos

LIST OF FIGURES

LIST OF ABBREVIATIONS

5-HT: serotonin

5-HT2C: serotonin receptor type 2C

ADHD: attention deficit hyperactivity disorder

AMPA: α-amino-3-hydroxy-5-methyl-4-isoxazolepropionic acid

ANOVA: analysis of variance

ASD: Autism Spectrum Disorder

C57BL/6J : C57 black 6J

Ca_v3.3: Voltage-gated calcium channel 3.3

DSI: direct social interaction test

EPMT: elevated plus-maze test

F: F-statistic value

Fig.: figure

Fmr1: Fragile X Mental Retardation 1

FMRP : Fragile X Mental Retardation Protein

g: gram

GABA: Gamma aminobutyric acid

GABAA: Gamma aminobutyric acid type A receptor

H: H-statistic value

kg: kilogram

KO: knockout

LTD: long term depression

M: molar

mA: milliamperes

mg: milligram

mGlur: metabotropic glutamate receptor

mL: milliliter

mm: millimeter

ms: millisecond

MT1: melatonin receptor type 1

MT2: melatonin receptor type 2

mTOR: mammalian target of rapamycin

nA: nanoamperes

NaCl: sodium chloride

NaOH: sodium hydroxide

NMDA: N-methyl-D-aspartate

OFT: open field test

p: probability

pH: potential of hydrogen

Ptchd1: Patched Domain Containing 1

REM: rapid eye motion

S1: stranger 1

S2: stranger 2

SEM: standard error of the mean

Shank3: SH3 and multiple ankyrin repeat domains 3

***Shank3*$^{-/-}$**: Shank3 homozygous knockout

***Shank3B*$^{-/-}$**: Shank3 subunit B homozygous knockout

SRIT: square root of the interaction time

SS: sum of squares

TCT: three chambers test

TRN: thalamic reticular nucleus

Tsc1: Tuberous Sclerosis Complex 1

Tsc2: Tuberous Sclerosis Complex 2

***Tsc2*$^{-/+}$**: Tsc2 heterozygous knockout

UCM924: N-[2-([3-bromophenyl]-4-fluorophenylamino)ethyl]acetamide

WT: wild type

η^2_{partial}: partial eta squared

1. INTRODUCTION

Despite its high prevalence, there is a lack of effective pharmacological treatment options that effectively alleviate the altered social behaviour in autism spectrum disorder (ASD) – one of its core symptoms and diagnostic criteria (Association, 2013). This, in part, is due to the highly heterogeneous nature of ASD. The aetiology of ASD can have a plethora of different genetic and biological underpinnings, which makes it especially difficult to identify pharmacological interventions that can correct such different pathophysiological processes. To this effect, identifying a common neurobiological impairment across multiple forms of ASD can help open the avenue to novel treatment options that target this common therapeutic target. Given the lack of selective pharmacologic interventions that effectively ameliorate the core symptoms of ASD, notably reduced social behaviour, the present study seeks to assess the effects of a novel melatonergic compound in three mouse models of ASD: *Fmr1* hemizygous KO, *Tsc2* heterozygous KO, and *Shank3* homozygous KO mice. Additionally, the electrophysiological properties of the thalamic reticular nucleus (TRN) are investigated as a potential common neurobiological dysfunction in these mouse models - assessing its validity as a therapeutic target in ASD. This brain region has been previously hypothesized to be implicated in ASD and other neurodevelopmental disorders (Krol, Wimmer, Halassa, & Feng, 2018), thus, we anticipated a dysfunction of TRN activity in these mouse models. Importantly, given the high expression of the MT2 receptor in the TRN (Lacoste et al., 2015) and that MT2 agonists have been shown to activate and regularize TRN activity (Ochoa-Sanchez et al., 2011), we hypothesize that if a dysfunction in TRN is found, that administration of the MT2 receptor agonist UCM924 will have a regularizing effect.

Aim 1: Characterization of behavioural phenotypes of three mouse models of ASD: To characterize the social behavior, anxiety-related behaviour, and locomotory phenotypes in the three strains of KO mice compared to their own wild type (WT) controls.

Aim 2: Characterizing electrophysiological properties of the TRN in mouse models of ASD: To identify differences in single-neuron firing and burst rate of TRN neurons in these mouse strains compared to WT controls. Additionally, to assess differences in firing rate responsivity to microiontophoretic ejections of quisqualate (excitatory) and GABA (inhibitory).

Aim 3: Testing a selective MT2 agonist in the reversal of behavioural and electrophysiological phenotypes of the mouse models of ASD: To the assess the effectiveness of UCM924, a novel selective MT2 partial agonist, in ameliorating the behavioural and TRN firing phenotypes identified in Aims 1 and 2. Additionally, to characterize its effects in WT mice.

REVIEW OF LITERATURE

1.1 *Autism Spectrum Disorder*

Autism spectrum disorder (ASD) is a prevalent neurodevelopmental disorder characterized by persistent deficits in social communication, social interaction, and repetitive patterns of behaviour (Association, 2013). Epidemiological studies assessing the prevalence of ASD have revealed a very high variability in their findings, in part due to differences in screening procedures and geographical location, with prevalence estimates typically ranging between 1 and 10 in 1000 (Chiarotti & Venerosi, 2020). Despite this relatively high prevalence, there is a lack of effective treatment options for individuals with ASD. Presently, existing off-label pharmacological treatments are used to mainly target some of the behavioural symptoms associated with ASD, such as hyperactivity, aggression, and self-injurious behaviour (LeClerc & Easley, 2015; Shenoy, Indla, & Reddy, 2017). For instance, antipsychotic medication has been shown to be effective in reducing irritability and aggression in children with ASD (Beherec et al., 2011; Remington, Sloman, Konstantareas, Parker, & Gow, 2001). However, existing research is limited and conflicting regarding the effectiveness of pharmacological intervention for social behaviour in ASD (Gencer et al., 2008; Miral et al., 2008). Given that deficits in social behaviour are core symptoms of ASD, there is an urgent need to identify novel prosocial agents that are effective in this population.

1.2 *Syndromes associated with autism spectrum disorder*

The aetiologies underlying a diagnosis of ASD, which can be genetic or non-genetic, are vastly heterogeneous, which explains the wide-ranging spectrum of symptom severity (Masi, DeMayo, Glozier, & Guastella, 2017). For instance, the variation in intelligence in children with ASD is much higher than that in neurotypical children (Billeiter & Froiland, 2022). Although the origin

of most ASD cases are not defined, the characterization of monogenic syndromes associated with ASD have contributed to the generation of preclinical models of ASD (Kazdoba et al., 2016), which recapitulate some of the behavioural and neurobiological phenotypes observed in human diagnoses.

1.21 *Fragile X Syndrome*

For example, Fragile X Syndrome is the most prevalent inherited form of ASD and is caused by the hyper-methylation of the fragile X mental retardation 1 (*Fmr1*) gene, located on the X chromosome. Upon its characterization, it was demonstrated that males or females can be premutation carriers (between 55 and 200 CGG repeats) or have the full mutation (greater than 200 CGG repeats) (Verkerk et al., 1991; Yu et al., 1991).This condition produces symptoms of greater severity in males, given that females receive compensation from the unaffected X chromosome (R. Hagerman, Au, & Hagerman, 2011). This mutation results in the loss of its downstream product, the fragile X mental retardation protein (FMRP) (R. J. Hagerman et al., 2017). FMRP is an important regulator of the translation of many mRNAs, thus, its absence results in abnormally high levels of protein synthesis (Napoli et al., 2008). Importantly, FMRP interacts with the transcripts of synaptic proteins, and others implicated in ASD (Darnell et al., 2011; Zalfa et al., 2003). Typically, Fragile X Syndrome is diagnosed around the age of 3 in children demonstrating delays in communication (Sureda, Alberca, & Navarro, 1991). Co-occurring symptoms in individuals with this condition include autism spectrum disorder, attention deficit hyperactivity disorder, anxiety, seizures, aggressiveness and self-harming behaviour (Bailey, Raspa, Olmsted, & Holiday, 2008).

This syndrome can be modeled preclinically with the *Fmr1* KO mouse, which has a loss-of-function mutation on the *Fmr1* gene resulting in the absence of FMRP. Despite this transgenic mouse line's existence for over 25 years ("Fmr1 knockout mice: a model to study fragile X mental retardation. The Dutch-Belgian Fragile X Consortium," 1994), there is still some inconsistency in the literature regarding the behavioural phenotypes of this mouse model, which is believed to be explained by the different genetic backgrounds of the transgenic strains (Kazdoba, Leach, Silverman, & Crawley, 2014; Spencer et al., 2011). Nevertheless, some of the more recurrent phenotypes include impaired social behaviour (Gantois et al., 2017) and decreased anxiety-related behaviour (Nolan et al., 2017; Sare, Levine, & Smith, 2016).

In addition to studying the behavioural phenotypes of these mice, the generation of this mouse line has allowed researchers to assess neurobiological abnormalities caused by the silencing of the *Fmr1* gene. For instance, FMRP is a negative regulator of metabotropic glutamate receptor 1 (mGluR1), a receptor with an important role in synaptic plasticity- notably long-term depression (LTD). Using *Fmr1* KO mice, it was confirmed that the loss of FMRP selectively enhances mGluR-mediated LTD in the hippocampus, bringing forth the "mGluR theory of fragile x syndrome" (Bear, Huber, & Warren, 2004; Huber, Gallagher, Warren, & Bear, 2002).

1.22 *Tuberous Sclerosis Complex*

Another prevalent genetic syndrome that can cause ASD is Tuberous Sclerosis Complex (Tsc) (Capal et al., 2021). Mutations to the *Tsc1* or *Tsc2* genes disrupt the production of their encoded proteins which regulate cell growth and metabolism via the mammalian target of rapamycin (mTOR) signalling (Orlova & Crino, 2010). *Tsc1* and *Tsc2* form heterodimers and are negative regulators of mTOR (Li, Corradetti, Inoki, & Guan, 2004). Individuals with Tuberous Sclerosis

Complex thus have an overactivation of mTOR, which often results in tumor-like lesions referred to as hamartomas, for which treatment with mTOR inhibitors are sometimes used (Curatolo & Moavero, 2012). As well, individuals with Tuberous Sclerosis Complex are often co-diagnosed with ASD (Capal et al., 2021). The implication of mTOR in ASD is well-documented, seeing how other genetic syndromes associated with ASD often manifest elevated levels of mTOR activity, including Fragile X Syndrome (Sharma et al., 2010).

This syndrome can be modelled preclinically with the *Tsc2* KO mouse line, which has been shown to display behavioural phenotypes similar to those manifested in clinical ASD diagnoses, such as reduced social behaviour (Sato et al., 2012) and increased levels of anxiety-related behaviour (Ehninger & Silva, 2011). In fact, *Tsc2* haploinsufficiency was demonstrated to be sufficient in producing ASD-like symptoms in rats (Waltereit, Japs, Schneider, de Vries, & Bartsch, 2011), such as reduced social behaviour. Interestingly, administration of an mTOR inhibitor was found to improve these symptoms, further suggesting an important role of mTOR in the pathogenesis of ASD (Petrasek et al., 2021).

1.23 *Shank3*

A third gene that, when mutated, can result in an ASD diagnosis is the SH3 and multiple ankyrin repeat domains 3 (*Shank3*) gene. *Shank3* encodes for an important synaptic scaffolding protein in the post-synaptic density, particularly implicated in excitatory neurotransmission (Moessner et al., 2007). For example, Shank3 proteins regulate AMPA and NMDA receptor-mediated synaptic transmission, and even regulate levels of presynaptic proteins via transsynaptic signaling (Arons et al., 2012). In humans, haploinsufficiency of the *Shank3* gene causes a condition known as

Phelan-McDermid syndrome, which is highly associated with ASD, among other distinct behavioural features such as impairments in verbal communication (Uchino & Waga, 2013).

This condition is modeled preclinically with the *Shank3* KO transgenic mouse line, which has been shown to exhibit ASD-like phenotypes, including impaired social behaviour, and synaptic dysfunction (Bozdagi et al., 2010; Peca et al., 2011). In fact, it was shown that *Shank3* knockdown in induced pluripotent stem cell-derived human neurons impaired neuronal development and spontaneous excitatory and inhibitory post synaptic currents (Huang et al., 2019).

1.3 *Thalamic reticular nucleus*

The thalamic reticular nucleus (TRN) is a thin sheet of gamma-aminobutyric acid- (GABA)-ergic neurons that exclusively send projections to other thalamic nuclei (Pinault, 2004). The connectivity between the TRN and thalamic nuclei is organized based on sensory modality, with subregions of the TRN projecting to distinct thalamic nuclei, which process and project these signals to corresponding cortical areas (Li et al., 2020). Among its afferent connections, the TRN receives input from primary sensory areas for which it serves as a gatekeeper of sensory information before this information is relayed through the thalamus and transmitted to higher-level processing areas; thus revealing an important role of the TRN in attentional processing (Zikopoulos & Barbas, 2006). Interestingly, it was recently discovered that the TRN can be further segregated into neuronal populations that are distinguished by the expression of a variety of genes that make up two distinct genetic profiles (Li et al., 2020). Furthermore, Li et al. (2020) found that the genetic profile classification of TRN neurons is highly correlated with the nature of their afferent projections: coming from first-order or higher-order cortical regions.

As well, the TRN has an important rhythmogenic role in sleep, notably in the generation of sleep spindles and slow wave oscillations (Vantomme, Osorio-Forero, Luthi, & Fernandez, 2019). For instance, optogenetic stimulation of a subset of TRN neurons is sufficient to produce endogenous-like sleep spindles (Thankachan et al., 2019). Importantly, the generation of sleep spindles are largely dependent on the activity of low threshold T-type calcium channels, encoded by the *$Ca_v3.3$* gene, which also mediate the burst firing activity of TRN neurons (Astori et al., 2011). In fact, the genetic inhibition of $Ca_v3.3$ channels in mice completely halted burst activity in TRN neurons, and also suppressed the rhythmogenesis of sleep spindles by disrupting non-REM sleep (Pellegrini, Lecci, Luthi, & Astori, 2016). As well, differences in sleep spindle activity have been demonstrated in humans with ASD compared to neurotypical individuals, such that the former have a lower density and duration of sleep spindles (Farmer et al., 2018; Merikanto et al., 2019).

Given the prevalence of atypical sensory processing (Marco, Hinkley, Hill, & Nagarajan, 2011) and sleep abnormalities (Devnani & Hegde, 2015) in individuals with ASD, phenomena in which the TRN is greatly implicated, it has recently been suggested that the TRN may be a reliable "circuit endophenotype" in neurodevelopmental disorders, notably ASD (Krol et al., 2018). In fact, the chemogenetic inhibition of a subset of TRN neurons was sufficient to impair prepulse inhibition (the phenomenon that a weaker prestimulus reduces the response of a reflex-eliciting stimulus), a phenomenon that is characteristically impaired in ASD (Perry, Minassian, Lopez, Maron, & Lincoln, 2007; You et al., 2021). As well, the deletion of the *Ptchd1* gene in mice, the mutation of which can cause ASD and intellectual disability in humans, impairs TRN activity and produces behavioural phenotypes such as intellectual impairment and aggression (Noor et al., 2010; Wells, Wimmer, Schmitt, Feng, & Halassa, 2016). Furthermore, Wells et al. (2016) showed that the TRN-specific deletion of *Ptchd1* resulted in deficits in attention and hyperactivity.

1.4 *Melatonergic compounds*

Many studies have demonstrated that individuals with ASD have lower levels of circulating melatonin and disrupted melatonin synthesis compared to healthy controls (Melke et al., 2008; Pagan et al., 2014; Tordjman et al., 2012). This plays a crucial role in the high prevalence of sleep abnormalities in individuals with ASD (Devnani & Hegde, 2015). In fact, sleep disturbances have even been found in the *Fmr1* KO and *Shank3* KO mouse models of ASD (Sare et al., 2017; Sare, Lemons, Song, & Smith, 2020). These findings have led to clinical trials assessing the therapeutic effects of melatonin supplementation in individuals with ASD, which have demonstrated that exogenous melatonin can improve sleep and help with some of the comorbidities of ASD, such as rigidity and anxiety (Garstang & Wallis, 2006; Rossignol & Frye, 2011). However, there is still a lack of selective medications that improve the core symptoms of ASD, notably reduced social behaviour.

Melatonin activates two G-protein coupled receptors, MT1 and MT2, which activate similar, but distinct signaling cascades (Cecon, Oishi, & Jockers, 2018). Briefly, both receptors are coupled to $G_{i/o}$-type proteins, while only MT2 is additionally coupled to G_q-type proteins (Jockers et al., 2016). One way in which this difference in signaling pathways is manifested functionally is the modulation of the GABAA receptor. Via MT1, melatonin potentiates the chloride current through the GABAA receptor while it inhibits this current via MT2 (Wan et al., 1999). Thus, one may hypothesize that neurons expressing both the GABAA and MT2 receptors will exhibit heightened activation in response to the administration of a MT2-selective agonist, given that the hyperpolarizing effect of the incoming chloride current (in response to GABAA activation) would be attenuated.

As a result of their difference in expression pattern and signaling cascades, MT1 and MT2 serve distinct mechanistic roles (Ng, Leong, Liang, & Paxinos, 2017). For instance, MT2 KO but not MT1 KO mice display reduced non-REM sleep compared to wild type controls, and the administration of an MT2 selective agonist in wild type mice is sufficient to enhance non-REM sleep (Ochoa-Sanchez et al., 2011). Furthermore, selective MT2 agonism has been shown to produce anxiolytic effects in mice (Ochoa-Sanchez et al., 2012). The same study also demonstrated that the anxiolytic effects of exogenous melatonin were blocked by a selective MT2 antagonist, suggesting that MT2 activation is sufficient to produce anxiolytic effects and necessary for the anxiolytic effects of melatonin. Interestingly, the MT2 receptor has recently been demonstrated to be implicated in social behaviour. Liu et al. (2017) showed that MT1/MT2 double KO and MT2 KO, but not MT1 KO mice displayed reduced social preference, suggesting the involvement of uniquely MT2 in the mediation of social behaviour (Liu, Clough, & Dubocovich, 2017). Conversely, Thomson et al. (2021) found that male MT2 KO mice exhibited increased social behaviour (Thomson, Mitchell, Openshaw, Pratt, & Morris, 2021). Although the nature of these conflicting findings should be explored in future studies, they are likely due to the different measures of social behaviour and the use of different genetic backgrounds which have different levels of endogenous melatonin (Goto, Oshima, Tomita, & Ebihara, 1989). Nevertheless, these findings, for the first time, highlight the role of MT2 in social behaviour. Neither of these studies explored the mechanism behind MT2's involvement in the mediation of social behaviour. The MT2 receptor is known to form functional heterodimers with the serotonin (5HT)-2C receptor, which is known to be involved in sociability (Kamal et al., 2015; Martin et al., 2014). Given the prevalence of anxiety as a comorbidity in individuals with ASD (Zaboski & Storch, 2018), in addition to this recent evidence of the involvement of MT2 and social behaviour (Thomson et al.,

2021), we sought to investigate the effects of UCM924, a novel selective MT2 partial agonist, in the *Fmr1* KO, *Tsc2* KO, and *Shank3* KO mouse models of ASD.

2. METHODOLOGY

2.1 *Drugs:*

UCM924 (N-[2-([3-bromophenyl]-4-fluorophenylamino)ethyl]acetamide) was dissolved in a vehicle (veh) solution made of 60% dimethylsulfoxide and 40% saline (0.9% solution) and delivered subcutaneously with a concentration of 6mg/mL at a dose of 20mg/kg body weight 2-3 hours before behavioural testing. For microiontophoretic applications, quisqualic acid (5mM) was dissolved in 200mM NaCl and titrated with NaOH until a final pH of 8 was achieved. Similarly, γ-Aminobutyric acid (GABA) (1M) was dissolved in 200mM NaCl and titrated in acetic acid until a final pH of 4 was achieved. Urethane (Sigma-Aldrich, Oakville, Canada) was used as an anesthetic for all electrophysiological experiments.

2.2 *In Vivo Electrophysiology:*

In vivo extracellular electrophysiological recordings were taken in the rostral thalamic reticular nucleus (TRN) as described in our lab's previous work (Inserra et al., 2021). Mice were anesthetized with urethane (1.2 g/kg, intra peritoneal) and placed on a stereotaxic apparatus. Anesthesia was monitored via toe pinch, assuring no reflexive movement occurred. Using a razor blade, the scalp was removed from behind the eyes until the back of the head. Next, a hand drill was used to remove the skull above the thalamic reticular nucleus, and a 1mm by 1mm window was made, exposing the brain. The rostral thalamic reticular nucleus was located using coordinates from the Franklin and Paxinos mouse brain atlas : −0.5 to −0.8 mm anteroposterior (AP) relative to Bregma, 0.8–1.2 mm mediolateral relative to the midline, 2.7–4 mm dorsoventral, relative to the dura mater. A single-barrelled glass pipettes filled with 2% Pontamine Sky Blue dissolved in 2M sodium acetate with a pH of 7.5 was fixed on a micro-positioner and lowered into the brain until

the TRN was located. TRN neurons were identified by their long burst (50ms) and accelerando-decelerando burst-firing pattern (Domich, Oakson, & Steriade, 1986). A burst was characterized as at least 4 action potentials with a maximum inter-spike interval of 20ms. At the end of each recording session, the recording site was marked by iontophoretic ejection (–530 mA, negative current for 10 minutes) of Pontamine Sky Blue for later histological verification of recording sites.

2.3 *Microiontophoresis:*

Extracellular recordings of the rostral TRN with microiontophoretic applications were taken as previously described (De Gregorio et al., 2021). The methodology for this technique was identical to that described in the section "in vivo electrophysiology", however, instead of a single-barreled electrode, a multi-barreled electrode with ionic solutions in the side barrels and the Pontamine Sky Blue- sodium acetate solution in the central barrel was used. We recorded the activity of single neurons in the TRN in response to increasing currents of quisqualate (ejected as an anion at currents of -20nA, -40nA, and -80nA, 50 second pulses) and GABA (ejected as a cation at currents of -20nA, -40nA, and -80nA, 50 second pulses). After a pulse of current, the firing rate of the neuron was left to stabilize before the next current was emitted.

2.4 *Direct Social Interaction Test:*

Test mice were placed in a clean transparent cage and left to habituate for 10 minutes. Immediately following the habituation, an unfamiliar age- and sex- matched C57BL/6J wild type stranger mouse was placed in the cage and the mice were left to freely engage in social interaction for 10 minutes. The interaction time was manually scored in blind offline and consisted of the following behaviours: nose-to-anogenital sniffing, nose-to-nose sniffing, social grooming, mounting, and close following.

2.5 *Three-Chamber Test:*

A three-chamber arena with openings between the chambers was used to assess sociability and preference for social novelty. Test mice were placed in the middle chamber and allowed to freely explore the empty three-chamber arena for 10 minutes. Immediately after habituation, an unfamiliar mouse (stranger 1, male C57BL/6J, age matched) was introduced into 1 of the 2 side chambers, enclosed in a wire cage, thus allowing only the test mouse to initiate social interaction. An identical empty wire cage was placed in the other side chamber. With this setup, the test mouse was again placed in the middle chamber and allowed to explore the three-chamber arena for 10 min. At the end of the 10-minute sociability test, a new unfamiliar mouse (stranger 2, male C57BL/6J, age matched) was placed in the previously unoccupied wire cage. The test mouse was observed for an additional 10 minutes to assess social novelty. The location of the empty wire cage was alternated between side chambers for different test mice to prevent chamber biases. Stranger 1 (S1) and 2 (S2) mice were always taken from separate home cages and counterbalanced for each side of the chamber apparatus and stranger cage. The time spent interacting with S1, S2, or the empty cage, was manually scored in blind. The interaction time was determined by measuring the duration of the head/body contacts or climbing of the subject mouse upon either the empty cage or the cage containing the stranger mouse In order to ensure a comparisons across treatments, strangers and genotype groups, and also to reduce the impact of variable exploration times between mice, we used a "sociability index" for each mouse, calculated as: 100 × (S1 interaction time− empty cage interaction time)/(S1 interaction time + empty cage interaction time) and a "social novelty index" for each mouse, calculated as: 100 × (S2 interaction time− S1 interaction time)/(S2 interaction time + S1 interaction time).

2.6 *Open field testing:*

Mice were individually placed at the center of a white-painted open field arena (40 x 40 x 15 cm) and left to explore the whole arena for 10 minutes. The experiment took place under standard room lighting. Anxiety-like thigmotactic ('wall-following') behavior was measured by the frequency and total duration of central zone (30 x 30 cm) visits, and locomotion was assessed via the total distance travelled during the test.

2.8 *Elevated Plus-Maze Test:*

Mice were placed in a cross-shaped, elevated (80 cm) maze consisting of 2 open (50 × 10 cm^2) and 2 walled (closed) (50 × 10 × 40 cm^3) arms, and behavior was recorded for 10 minutes. Mice were singly placed in the central platform facing the open arm, and the following measures were collected using a motion-tracking software: time spent in the open arms, number of entries to the open arm, and total distance travelled.

2.9 *Timeline of experiments*

On day 1, mice were administered vehicle or UCM924 2-3 hours before undergoing the DSI, EPMT, and the OFT, in that order. On day 2, mice were administered the same treatment as they did on day 1, 2-3 hours before undergoing the TCT. Following a wash-out period of at least 2 weeks, some of these mice underwent electrophysiology or microiontophoresis experiments.

2.10 *Statistical Analysis:*

For two-factor between-subject designs, data underwent the Shapiro-Wilks test and the Levene's test in order to assess the assumptions of normality and of homogeneity of variance, respectfully. If these assumptions were not violated, then a two-way between subject ANOVA was performed, with "statistical significance" occurring when the p-value is less than 0.05. When necessary, post

hoc Tukey's comparisons were used. If one of the assumptions were not met, a square root transformation was performed and these new data were re-assessed for the violations of normality and homogeneity of variance. Square root transformations were performed in Microsoft excel by taking the square root of each value. For two-factor mixed designs, data was corrected for unequal sphericity using the Greenhouse-Geisser correction. For one-factor between subject designs, the normality and homogeneity of variance assumptions were tested. If these were not violated, a one-way ANOVA was performed. If one of the assumptions was violated, a Kruskal-Wallis test was be performed. In this nonparametric case, post hoc Mann-Whitney tests with Bonferroni correction were used. The abovementioned statistical analyses were performed with the statistical programs ANOVA1 2020, ANOVA2 2020, NormCheck_R 2020, and QuickUW 2020 (created by Dr. Joseph Rochford at McGill University, for all parametric analyses), and SPSS (for non-parametric analyses). Graphs were created using GraphPad Prism.

3. Research Findings

3.1 *Fmr1* KO:

3.11 *Social Behaviour:*

We first performed the Direct Social Interaction Test and compared the interaction time between groups. Given that the data were not normally distributed, a square root transformation was performed. A two factor (Treatment x Genotype) between subject ANOVA conducted on the transformed data yielded a significant main effect of genotype (genotype: $F(1,44)=6.41$, $p=0.015$; treatment: $F(1,44)=0.91$, $p>0.05$; interaction: $F(1,44)=1.55$, $p>0.05$) such that the square root of the interaction time (SRIT) of the *Fmr1* KO mice was less than that of the WT mice (Fig. 1A).

Next, we performed the Three-Chamber Test and assessed differences in sociability indices and in social novelty indices. A two factor (Genotype x Treatment) between subject ANOVA performed on the sociability indices revealed a trend towards a significant genotype x treatment interaction (genotype: $F(1,43)=2.5$, $p>0.05$; treatment: $F(1,43)=4.0$, $p=0.052$; interaction: $F(1,43)=3.79$, $p=0.058$; Fig. 1B). No significant differences were found in the omnibus two-way ANOVA of the social novelty indices (genotype: $F(1,41)=0.96$, $p>0.05$; treatment: $F(1,41)=0.37$, $p>0.05$; interaction: $F(1,41)=0.015$, $p>0.05$; Fig. 1C).

3.12 *Anxiety-related behaviour:*

Next, we performed the elevated plus maze test (EPMT) and the open field test (OFT) to assess anxiety-like behaviour. First, a two way between subject ANOVA performed on the open arm time data from the EPMT revealed a trend towards a main effect of genotype (genotype: $F(1,45) = 3.61$, $p=0.064$; treatment: $F(1,45)=0.19$, $p>0.05$; interaction: $F(1,45)=0.15$, $p>0.05$) such that KO mice

tended to spend more time on the open arm (Fig. 1D). Next, we assessed the distance travelled in the EPMT. A two factor between subject ANOVA revealed a significant main effect of genotype (genotype: $F(1,45) = 18.54$, $p<0.0001$; treatment: $F(1,45)=3.08$, $p>0.05$; interaction: $F(1,45)=0.24$, $p>0.05$) such that KO mice travelled significantly more than WT mice (Fig. 1E). No significant differences were found in the entries to open arm (analyzed as the square root of the number of entries; genotype: $F(1,45)=0.83$, $p>0.05$; treatment: $F(1,45)=0.033$, $p>0.05$; interaction: $F(1,45)=0.38$, $p>0.05$), of the EPMT. In the OFT, no significant differences were found in the distance travelled (genotype: $F(1,14)=0.14$, $p>0.05$; treatment: $F(1,14)=0.70$, $p>0.05$; interaction: $F(1,45)=0.45$, $p>0.05$; Fig. 1H), time in center (analyzed as the square root of the time in center; genotype: $F(1,22)=0.0023$, $p>0.05$; treatment: $F(1,22)=0.046$, $p>0.05$; interaction: $F(1,22)=1.81$, $p>0.05$; Fig. 1G), and entries to center (genotype: $F(1,22)=0.0$, $p>0.05$, treatment: $F(1,22)=0.64$, $p>0.05$; interaction: $F(1,22)=1.62$, $p>0.05$; Fig. 1H).

3.13 *Electrophysiology and microiontophoresis:*

Next, we performed in vivo single-unit extracellular recordings to assess differences in firing rate (spikes per second) and burst rate (bursts in 100 seconds) between WT, KO, and KO mice treated with UCM924. A one factor independent samples Kruskal-Wallis test revealed a significant effect of condition on the firing rate ($H(2) = 23.706$, $p<0.001$, Fig. 1I). Post hoc Mann-Whitney tests with Bonferroni correction revealed a trend that the firing rate of KO mice was lower than that of WT mice, however this difference was not statistically significant after Bonferroni correction ($p=0.040$, critical p-value = 0.017), and also that UCM924 significantly increased the firing rate in KO mice ($p<0.001$). The same analysis was performed on the burst rate, and a one factor Kruskal-Wallis test revealed a significant effect of condition ($H(2) = 26.321$, $p<0.001$, Fig. 1J).

Post hoc analyses revealed no significant difference between KO mice compared to the WT mice ($p=0.234$), but that UCM924 significantly increased the burst rate in the KO mice ($p<0.001$).

We subsequently performed microiontophoresis experiments to assess differences in firing rate response to ejections of quisqualate and GABA. For the ejections of quisqualate, a two factor (genotype x current) mixed design ANOVA with Greenhouse-Geisser correction was performed on the % baseline firing rate data, which revealed a significant main effect of current (current: $F(1.363, 28.615) = 18.42$, $p<0.001$; genotype: $F(1,21)=0.26$, $p>0.05$; interaction: $F(1.363, 28.615)=0.97$, $p>0.05$; Fig. 1K). Post hoc Dunnett contrasts revealed that the firing rate in response to 80nA of current was significantly higher than that of 0nA of current ($p<0.001$). We then performed a two factor mixed design ANOVA on the firing rate response to ejections of GABA, which similarly revealed a significant main effect of current ($F(2.042, 40.84) = 82.44$, $p<0.001$, genotype: $F(1,20)=3.08$, $p=0.0948$; interaction: $F(2.042,40.84)=2.27$, $p>0.05$); Fig. 1L). Post hoc analyses revealed that the firing rate response of 20nA ($p<0.001$), 40nA ($p<0.001$), and 80nA ($p<0.001$), of current were significantly lower than that of 0nA.

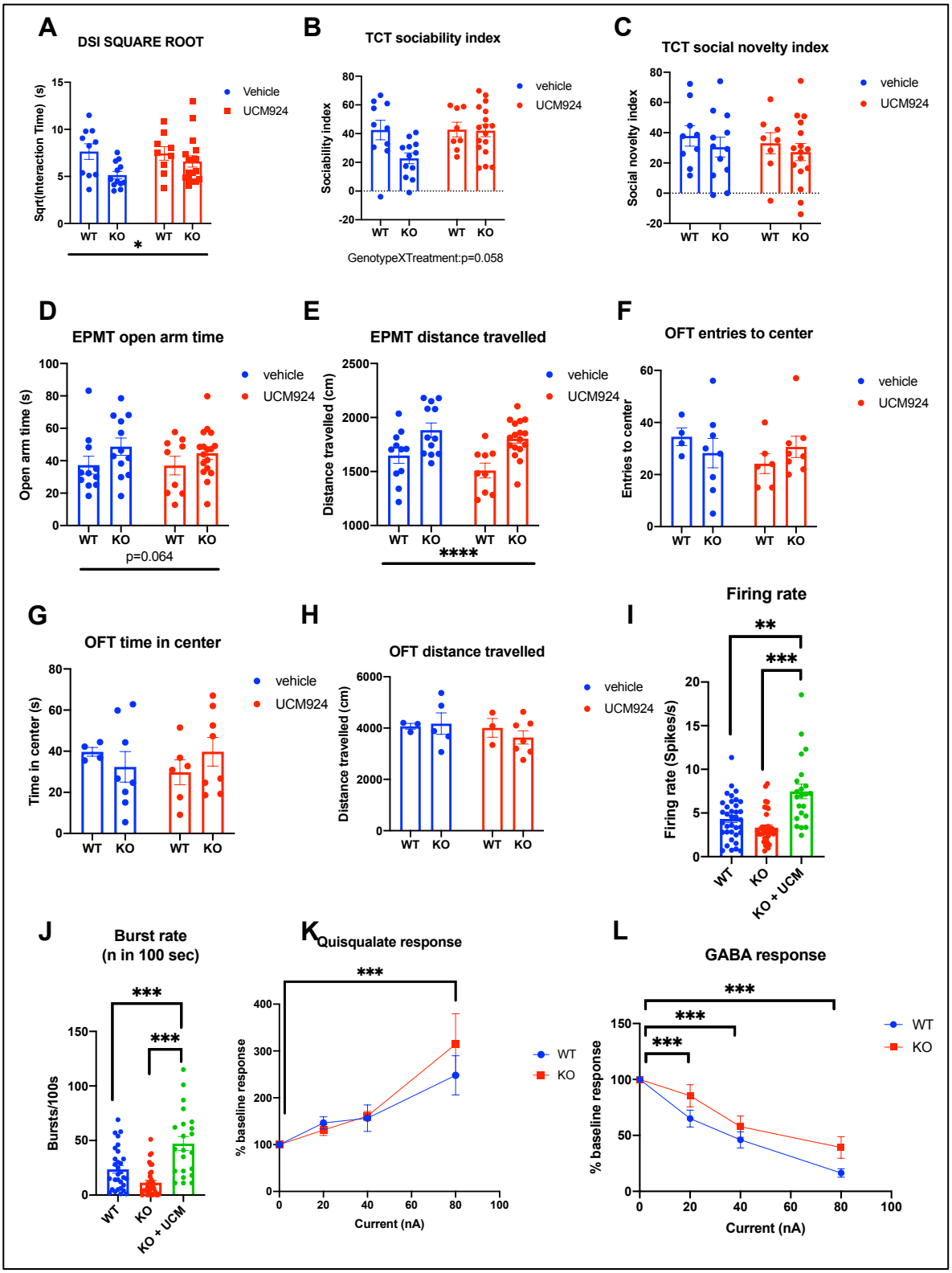
A
DSI SQUARE ROOT
Sqrt(Interaction Time) (s)
Vehicle
UCM924
WT KO WT KO
*
B
TCT sociability index
Sociability index
vehicle
UCM924
WT KO WT KO
GenotypeXTreatment:p=0.058
C
TCT social novelty index
Social novelty index
vehicle
UCM924
WT KO WT KO
D
EPMT open arm time
Open arm time (s)
vehicle
UCM924
WT KO WT KO
p=0.064
E
EPMT distance travelled
Distance travelled (cm)
vehicle
UCM924
WT KO WT KO
****
F
OFT entries to center
Entries to center
vehicle
UCM924
WT KO WT KO
G
OFT time in center
Time in center (s)
vehicle
UCM924
WT KO WT KO
H
OFT distance travelled
Distance travelled (cm)
vehicle
UCM924
WT KO WT KO
I
Firing rate
**
***
Firing rate (Spikes/s)
vehicle
UCM924
WT KO KO + UCM
J
Burst rate
(n in 100 sec)
***
***
Bursts/100s
WT KO KO + UCM
K
Quisqualate response
***
% baseline response
WT
KO
Current (nA)
L
GABA response
***
***
***
% baseline response
WT
KO
Current (nA)

Figure 1: Behavioural and electrophysiological results in *Fmr1* KO mice and effects of UCM924

A) Direct social interaction test results. The data were analyzed as the square root of the interaction time (n= 9-17 mice) B) Sociability phase of the three chambers test. The data were transformed to a sociability index by the following formula: 100 x (time spent sniffing stranger mouse 1 – time spent sniffing empty cage) / (time spent sniffing stranger mouse 1 + time spent sniffing empty cage) (n= 8-17 mice). C) Social novelty phase of the three chambers test. The data were transformed to a social novelty index by the following formula: 100 x (time spent sniffing stranger mouse 2 – time spent sniffing stranger mouse 1) / (time spent sniffing stranger mouse 2 + time spent sniffing stranger mouse 1) (n= 8-17 mice). D) Time spent on the open arm during the elevated plus maze test (n= 9-17 mice). E) Total distance travelled during the elevated plus maze test (n= 9-17 mice). F) Total number of entries to the center of the open field test (n= 4-8 mice). G) Total time in the center of the open field test (n= 4-8 mice). H) Total distance travelled during the open field test (n= 3-7 mice). I) Spontaneous firing rate (spikes/second) of TRN neurons. (n= 2-4 mice, 22-36 neurons). J) Burst rate (number of bursts in 100 seconds) of TRN neurons (n= 2-4 mice, 22-36 neurons). K) Firing rate response to microiontophoretic ejections of quisqualate (20nA, 40nA, 80nA), analyzed as % baseline response (n= 4-5 mice, 10-13 neurons). L) Firing rate response to microiontophoretic ejections of GABA (20nA, 40nA, 80nA), analyzed as % baseline response (n= 4-5 mice, 10-12 neurons). All data are presented as mean ± SEM. For A-H, two-way between-subject ANOVA with post hoc Tukey tests were performed. For I-J, a Kruskal Wallis test was performed with post hoc Mann-Whitney comparisons with Bonferroni correction. For K-L, two-way mixed-factor ANOVA with Greenhouse-Geisser correction was performed, with post hoc Dunnett contrasts (comparing group means to the current=0nA condition). No symbol = n.s., * $p<0.05$, ** $p<0.01$, ***$p<0.001$, ****$p<0.0001$. For 2-way ANOVA: symbols on

horizontal lines under the graph represent main effect of genotype, symbols beside vertical lines to the upper-right of the graph indicate main effect of treatment, symbols above two distinct groups represent interaction effects.

3.2 Tsc2 KO:

3.21 *Social Behaviour:*

We performed a two way between subject ANOVA on the square root of the interaction time (SRIT) of the direct social interaction test (the original data were not normally distributed), which revealed a significant main effect of treatment such that mice treated with UCM924 had a significantly higher SRIT than vehicle-treated mice (genotype: $F(1,46)=2.92$, $p>0.05$; treatment: $F(1, 46) = 7.09$, $p<0.05$; interaction: $F(1,46)=1.01$, $p>0.05$; Fig. 2A). We also performed a two way between subject ANOVA for the sociability index (underwent a square root transformation, genotype: $F(1,36)=0.98$, $p>0.05$; treatment: $F(1,36)=0.31$, $p>0.05$; interaction: $F(1,36)=0.024$, $p>0.05$; Fig. 2B) and the social novelty index (genotype: $F(1,36)=0.54$, $p>0.05$; treatment: $F(1,36)=0.001$, $p>0.05$; interaction: $F(1,36)=0.004$, $p>0.05$; Fig. 2C) of the TCT, in which no significant differences were found.

3.22 *Anxiety-related behaviour:*

We first analyzed the measures acquired from the EPMT. A two way between subject ANOVA performed on the open arm time revealed a trend towards a main effect of treatment (genotype: $F(1,36)=0.56$, $p>0.05$; treatment: $F(1,36) = 4.06$, $p=0.052$; interaction: $F(1,36)=0.56$, $p>0.05$; Fig. 2D) such that mice receiving UCM924 tended to spend more time in the open arm than mice treated with vehicle. The same analysis was performed on the distance travelled in the EPMT (Fig.

2E), which revealed a significant main effect of treatment such that mice receiving UCM924 travelled significantly more than those receiving vehicle (genotype $F(1,36)=0.009$, $p>0.05$; treatment: $F(1,36) = 9.78$, $p <0.01$; interaction: $F(1,36)=0.015$, $p>0.05$). No significant differences were found in omnibus two factor between subject ANOVA for the number of entries to the open arm (genotype $F(1,36)=0.064$, $p>0.05$; treatment: $F(1,36) =0.17$, $p >0.05$; interaction: $F(1,36)=0.064$, $p>0.05$).

In the OFT (Fig. 2F-H), no significant differences were found in the omnibus two way between subject ANOVA for the number of entries to center (analyzed as the square root of the number of entries, genotype: $F(1,26)=1.04$, $p>0.05$; treatment: $F(1,26) =1.80$, $p >0.05$; interaction: $F(1,26)=3.43$, $p>0.05$), time in center (genotype: $F(1,26)=0.59$, $p>0.05$; treatment: $F(1,26) =0.40$, $p >0.05$; interaction: $F(1,26)=4.18$, $p>0.05$), nor in the distance travelled (genotype: $F(1,17)=0.0023$, $p>0.05$; treatment: $F(1,17) =2.65$, $p >0.05$; interaction: $F(1,26)=0.062$, $p>0.05$).

3.33 *Electrophysiology and microiontophoresis:*

Next, we took in vivo single-unit extracellular recordings to assess differences in TRN firing and burst rate. A Kruskal-Wallis test was performed on the firing rate data revealed a significant main effects for firing rate ($H(2)=38.586$, $p<0.001$, Fig. 2I). Post hoc Mann-Whitney tests with Bonferroni correction revealed that KO mice had significantly lower firing rate than WT mice ($p<0.001$), and that UCM924 significantly increased the firing rate in KO mice ($p<0.001$). Similarly, a Kruskal-Wallis test was employed on the burst rate data, which revealed a significant effect ($H(2) = 29.108$, $p<0.001$, Fig. 2J). Post hoc Mann-Whitney tests with Bonferroni correction revealed that KO mice had significantly lower burst rate than WT mice ($p<0.001$), and that UCM924 significantly increased the burst rate in KO mice ($p<0.001$).

We then performed electrophysiological recordings with micrioniontophoretic ejections. For ejections of quisqualate, a two-way mixed factor ANOVAs performed on the firing rate date revealed a significant main effect of current (current: $F(1.27,26.65) = 14.58$, $p<0.001$; genotype: $F(1,21)=0.0065$, $p>0.05$; interaction: $F(1.27,26.65)=0.10$, $p>0.05$; Fig. 2K). Post hoc Dunnett contrasts revealed that the firing rate in response to 40nA ($p<0.01$) and 80nA ($p<0.001$) of current was significantly higher than that of 0nA of current.

A two-way mixed factor ANOVA was subsequently performed on the firing rate data in response to microiontophoretic ejections of GABA, which revealed a significant main effect of current (current: $F(2.03,44.65)=131.53$, $p<0.001$; genotype: $F(1,22)=0.037$, $p>0.05$; interaction: $F(2.03,44.65)=0.22$, $p>0.05$; Fig. 2L). Post hoc Dunnett contrasts revealed that the firing rate in response to 20nA ($p<0.001$), 40nA ($p<0.001$) and 80nA ($p<0.001$) of current was significantly lower than that of 0nA of current.

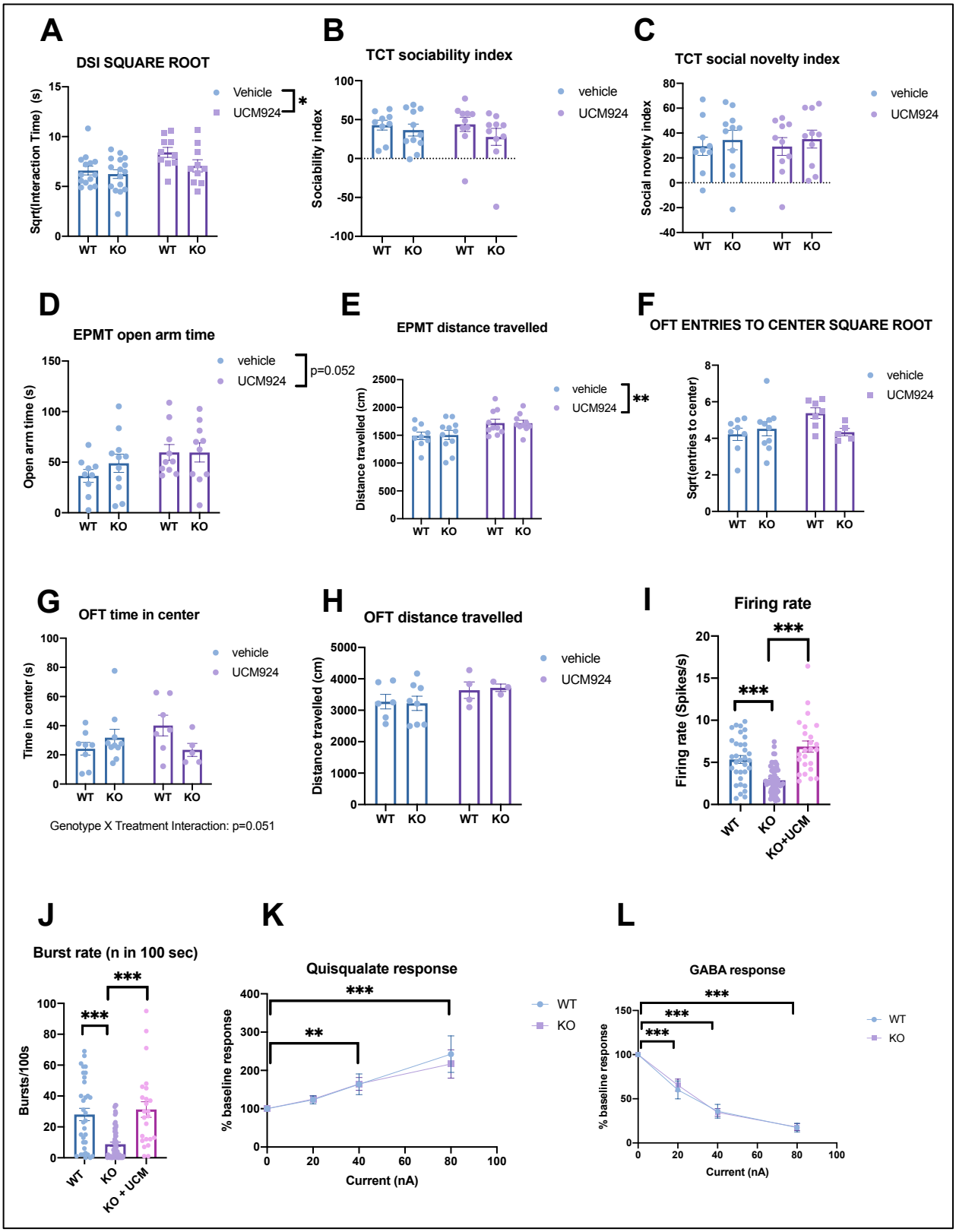
A
DSI SQUARE ROOT
Sqrt(Interaction Time) (s)
Vehicle
UCM924
*
WT KO WT KO
B
TCT sociability index
Sociability index
vehicle
UCM924
WT KO WT KO
C
TCT social novelty index
Social novelty index
vehicle
UCM924
WT KO WT KO
D
EPMT open arm time
Open arm time (s)
vehicle
UCM924
p=0.052
WT KO WT KO
E
EPMT distance travelled
Distance travelled (cm)
vehicle
UCM924
**
WT KO WT KO
F
OFT ENTRIES TO CENTER SQUARE ROOT
Sqrt(entries to center)
vehicle
UCM924
WT KO WT KO
G
OFT time in center
Time in center (s)
vehicle
UCM924
WT KO WT KO
Genotype X Treatment Interaction: p=0.051
H
OFT distance travelled
Distance travelled (cm)
vehicle
UCM924
WT KO WT KO
I
Firing rate
Firing rate (Spikes/s)
***
***
WT KO KO+UCM
J
Burst rate (n in 100 sec)
Bursts/100s
***
***
WT KO KO + UCM
K
Quisqualate response
% baseline response
***
**
WT
KO
Current (nA)
L
GABA response
% baseline response
***
***
***
WT
KO
Current (nA)

Figure 2: Behavioural and electrophysiological results in *Tsc2* KO mice and effects of UCM924

A) Direct social interaction test results. The data were analyzed as the square root of the interaction time (n=10-16 mice). B) Sociability phase of the three chambers test. The data were transformed to a sociability index by the following formula: 100 x (time spent sniffing stranger mouse 1 – time spent sniffing empty cage) / (time spent sniffing stranger mouse 1 + time spent sniffing empty cage) (n=9-11 mice). C) Social novelty phase of the three chambers test. The data were transformed to a social novelty index by the following formula: 100 x (time spent sniffing stranger mouse 2 – time spent sniffing stranger mouse 1) / (time spent sniffing stranger mouse 2 + time spent sniffing stranger mouse 1) (n=9-11 mice). D) Time spent on the open arm during the elevated plus maze test (n=9-11 mice). E) Total distance travelled during the elevated plus maze test (n=9-11 mice). F) Total number of entries to the center of the open field test. Analyzed as the square root of the total number of entries (n=5-10 mice). G) Total time in the center of the open field test (n=5-10 mice). H) Total distance travelled during the open field test (n=3-8 mice). I) Spontaneous firing rate (spikes/second) of TRN neurons (n= 3-4 mice, 33-60 neurons). J) Burst rate (number of bursts in 100 seconds) of TRN neurons (n= 3-4 mice, 33-60 neurons). K) Firing rate response to microiontophoretic ejections of quisqualate (20nA, 40nA, 80nA), analyzed as % baseline response (n= 2-5 mice, 8-15 neurons). L) Firing rate response to microiontophoretic ejections of GABA (20nA, 40nA, 80nA), analyzed as % baseline response (n= 2-5 mice, 8-16 neurons). All data are presented as mean ± SEM. For A-H, two-way between-subject ANOVA with post hoc Tukey tests were performed. For I-J, a Kruskal Wallis test was performed with post hoc Mann-Whitney comparisons with Bonferroni correction. For K-L, two-way mixed-factor ANOVA with Greenhouse-Geisser correction was performed, with post hoc Dunnett contrasts (comparing group means to the current=0nA condition). No symbol = n.s., * $p<0.05$, ** $p<0.01$, ***$p<0.001$,

****p<0.0001. For 2-way ANOVA: symbols on horizontal lines under the graph represent main effect of genotype, symbols beside vertical lines to the upper-right of the graph indicate main effect of treatment, symbols above two distinct groups represent interaction effects.

3.3 Shank3 KO:

3.31 *Social Behaviour:*

We first assessed social behaviour in the *Shank3* mice by performing the DSI and the TCT. Two-way between subject ANOVAs were performed on the square root of the DSI data (genotype: $F(1,44)=0.46$, $p>0.05$; treatment: $F(1,44)=0.27$, $p>0.05$; interaction: $F(1,44)=0.68$, $p>0.05$; Fig. 3A), on the sociability index of the TCT (genotype: $F(1,44)=2.04$, $p>0.05$; treatment: $F(1,44)=0.68$, $p>0.05$; interaction: $F(1,44)=0.068$, $p>0.05$; Fig. 3B), and on the social novelty index of the TCT (genotype: $F(1,44)=2.15$, $p>0.05$; treatment: $F(1,44)=3.76$, $p>0.05$; interaction: $F(1,44)=1.11$, $p>0.05$; Fig. 3C) and revealed no significant differences between groups. However, a trend ($p=0.059$) was found in the treatment effect of the social novelty index, such that mice treated with UCM924 tended to have a higher social novelty index than vehicle-treated mice.

3.32 *Anxiety-related behaviour:*

We then performed the EPMT, OFT, and the LDBT to assess differences in anxiety-related behaviour.

No significant differences were found in the two-way between subject ANOVAs for the EPMT metrics: open arm time (analyzed as the square root of the open arm time; genotype: $F(1,44)=1.30$, $p>0.05$; treatment: $F(1,44)=0.84$, $p>0.05$; interaction: $F(1,44)=0.0044$, $p>0.05$; Fig. 3D), number of entries to the open arm (genotype: $F(1,44)=0.62$, $p>0.05$; treatment: $F(1,44)=1.75$, $p>0.05$;

interaction: $F(1,44)=1.05$, $p>0.05$), and distance travelled (genotype: $F(1,44)=2.04$, $p>0.05$; treatment: $F(1,44)=1.57$, $p>0.05$; interaction: $F(1,44)=0.26$, $p>0.05$; Fig. 3E).

For the OFT (Fig. 3F-H), first, a two-way between subject ANOVA performed on the distance travelled revealed a significant main effect of genotype (genotype: $F(1,15)=6.16$, $p=0.025$; treatment: $F(1,15)=0.71$, $p>0.05$; interaction: $F(1,15)=1.71$, $p>0.05$), such that KO mice travelled a significantly smaller distance than WT mice. Next, the same analysis was performed on the square root of the number of entries to the center (genotype: $F(1,33)=14.32$, $p<0.001$; treatment: $F(1,33)=0.21$, $p>0.05$; interaction: $F(1,33)=1.04$, $p>0.05$) and on the square root of the time in the center of the OFT (genotype: $F(1,33)=6.20$, $p<0.05$; treatment: $F(1,33)=1.33$, $p>0.05$; interaction: $F(1,15)=1.90$, $p>0.05$), which revealed a significant main effect of genotype for both, such that KO mice had less entries to and time in the center (square root of the data).

3.33 *Electrophysiology*:

Finally, we took in vivo single-unit recordings of TRN neurons in these mice. A one-way between subject ANOVA on the firing rate data revealed a significant main effect ($F(2,124)=13.89$, $p<0.0001$, Fig. 3J). Post hoc Tukey comparisons revealed that the firing rate of KO mice was significantly higher than WT mice ($p<0.0001$), and that UCM924 significantly decreased the firing rate in KO mice ($p<0.05$). Similarly, a Kruskal-Wallis test performed on the burst rate data revealed a significant main effect ($H(2)= 9.678$, $p<0.01$, Fig. 3K). Post hoc Mann-Whitney tests with Bonferroni correction revealed that KO mice had a significantly higher burst rate than WT mice ($p<0.01$).

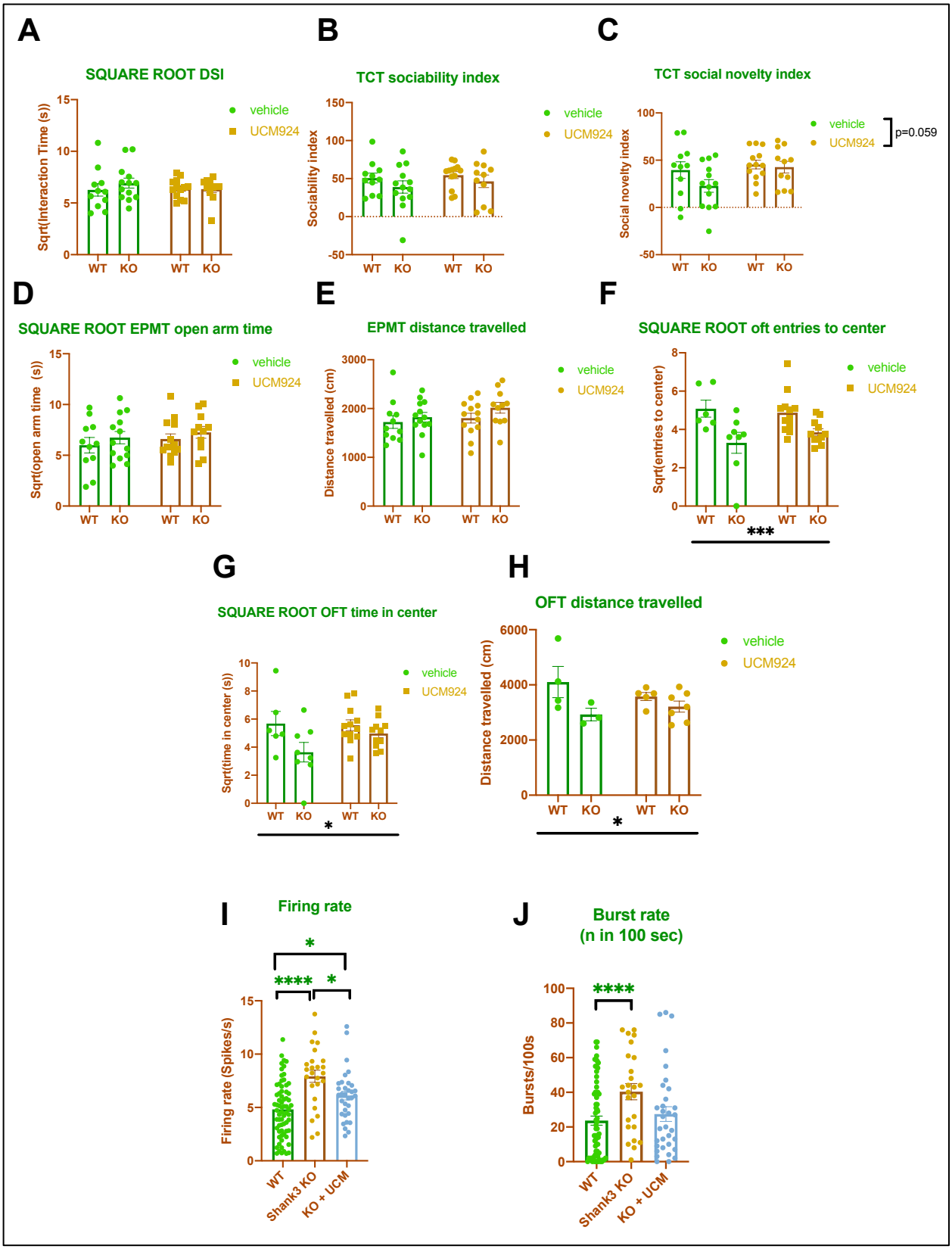
A
SQUARE ROOT DSI
Sqrt(Interaction Time (s))
vehicle
UCM924
WT KO WT KO
B
TCT sociability index
Sociability index
C
TCT social novelty index
Social novelty index
p=0.059
D
SQUARE ROOT EPMT open arm time
Sqrt(open arm time (s))
E
EPMT distance travelled
Distance travelled (cm)
F
SQUARE ROOT oft entries to center
Sqrt(entries to center)
***
G
SQUARE ROOT OFT time in center
Sqrt(time in center (s))
*
H
OFT distance travelled
Distance travelled (cm)
*
I
Firing rate
Firing rate (Spikes/s)
*
****
*
WT
Shank3 KO
KO + UCM
J
Burst rate
(n in 100 sec)
Bursts/100s
****

Figure 3: Behavioural and electrophysiological results in *Shank3* KO mice and effects of UCM924

A) Direct social interaction test results. The data were analyzed as the square root of the interaction time (n= 11-13 mice). B) Sociability phase of the three chambers test. The data were transformed to a sociability index by the following formula: 100 x (time spent sniffing stranger mouse 1 – time spent sniffing empty cage) / (time spent sniffing stranger mouse 1 + time spent sniffing empty cage) (n= 11-13 mice). C) Social novelty phase of the three chambers test. The data were transformed to a social novelty index by the following formula: 100 x (time spent sniffing stranger mouse 2 – time spent sniffing stranger mouse 1) / (time spent sniffing stranger mouse 2 + time spent sniffing stranger mouse 1) (n= 11-13 mice). D) Time spent on the open arm during the elevated plus maze test. Analyzed as the square root of the time on the open arm (n= 11-13 mice). E) Total distance travelled during the elevated plus maze test (n= 11-13 mice). F) Total number of entries to the center of the open field test. Analyzed as the square root of the total number of entries (n= 6-12 mice). G) Total time in the center of the open field test. Analyzed as the square root of the total time in the center (n= 6-12 mice). H) Total distance travelled during the open field test (n= 3-7 mice). I) Spontaneous firing rate (spikes/second) of TRN neurons (n= 3-8 mice, 25-69 neurons). J) Burst rate (number of bursts in 100 seconds) of TRN neurons (n= 3-8 mice, 25-69 neurons). All data are presented as mean ± SEM. For A-H, two-way between-subject ANOVA with post hoc Tukey tests were performed. For I, a one-way between-subejct ANOVA with post hoc Tukey tests was performed. For J, a Kruskal Wallis test was performed with post hoc Mann-Whitney comparisons with Bonferroni correction. No symbol = n.s., * $p<0.05$, ** $p<0.01$, ***$p<0.001$, ****$p<0.0001$. For 2-way ANOVA: symbols on horizontal lines under the graph represent main effect of genotype, symbols beside vertical lines to the upper-right of the graph indicate main effect of treatment, symbols above two distinct groups represent interaction effects.

4. Discussion

4.1 *Behavioural phenotypes:*

Firstly, *Fmr1* KO mice displayed reduced social behaviour in the Direct Social Interaction Test and a trend of reduced social preference in the Three Chambers Test. These results are in line with previous research demonstrating a robust anti-social phenotype in this transgenic mouse line (Gantois et al., 2017; Hebert et al., 2014; McNaughton et al., 2008). Importantly, these findings in particular further validate this preclinical model of ASD; given that reduced social interest is one of the main diagnostic criteria (Association, 2013). In our experimental setting, the *Tsc2* and *Shank3* KO mice did not exhibit any differences in social behaviour, which deviates from the previous literature (Chevere-Torres, Maki, Santini, & Klann, 2012; Peca et al., 2011; Sato et al., 2012). One potential explanation for this finding could be the use of slightly different genotypes of the mice tested. For instance, Chevere-Torres et al. found an antisocial phenotype in mice expressing a dominant/negative Tsc2 protein, which is different from the loss-of-function mutation of the *Tsc2*$^{-/+}$ mice used in the present study. Sato et al. (2012) also found an antisocial phenotype in *Tsc*$^{-/+}$ mice, however, our methodology for the Direct Social Interaction Test was different from theirs: they performed the test in the home cage of the test mouse whereas we performed it in a new cage, perhaps introducing a factor of stress. This additional stress might interact with differential stress responses between WT and KO mice, in which case there may only be a difference in social behaviour between genotypes under a condition of stress. Furthermore, Peca et al. (2011) found an antisocial phenotype in *Shank3B*$^{-/-}$ mice, however we used canonical *Shank3*$^{-/-}$ mutant mice. Thus, perhaps inhibiting different portions of the Shank3 gene causes distinct behavioural phenotypes.

Next, *Fmr1* KO mice exhibited a trend of reduced anxiety-like behaviour (demonstrated by an increased time in the open arm of the Elevated Plus Maze Test). Although this is contrary to the typical phenotype observed in humans with ASD that generally display increased levels of anxiety (Zaboski & Storch, 2018), these findings are consistent with others in the literature that found an increased time in the open arm of the EPMT (Nolan et al., 2017; Sare et al., 2016). As well, the *Fmr1* KO mice had an increased distance travelled in the EPMT compared to the WT mice. Since no differences were found in the distance travelled in the OFT, this finding in the EPMT might not necessarily reflect a phenotypic difference in locomotion, but rather another demonstration of reduced anxiety while undergoing the anxiogenic environment of the EPMT. However, previous research has found that *Fmr1* KO mice are, in fact, hyperactive (Nolan et al., 2017; Sare et al., 2016). *Tsc2* KO mice did not display differences in anxiety-related behaviour. There is some inconsistency in the literature regarding transgenic *Tsc2* mouse lines, with some studies demonstrating no differences in anxiety-like behaviour in heterozygous Tsc2 loss-of-function mutations (Ehninger et al., 2008), and others showing varying anxiety-related phenotypes in more specific mutations of the *Tsc2* gene (Ehninger & Silva, 2011; Yuan et al., 2012). However, the present findings are consistent with those in the former which used the same heterozygous KO mice. The *Shank3* KO mice did not display any differences in the EPMT, but spent less time and had fewer entries to the center of the open field than WT mice. They also had a smaller distance travelled in the OFT, suggesting a locomotor impairment. It has been previously shown that *Shank3* KO mice on a C57Bl/6 background exhibit less entries to the center of the open field (and a trend for less time in the center) (Drapeau, Dorr, Elder, & Buxbaum, 2014). However, the same study also found differences in the time spent in the open arm of the elevated zero maze test, whereas we found no such difference in the EPMT.

4.2 *Thalamic reticular nucleus activity:*

While the *Tsc2* KO and *Shank3* KO mice displayed statistically significant differences in firing rate and burst rate compared to their corresponding wild types, the *Fmr1* KO mice showed a trend of decreased firing rate compared to their corresponding wild type mice (statistical significance that did not survive Bonferroni correction). Interestingly, the *Fmr1* KO and *Tsc2* KO mice displayed reduced spontaneous firing and burst rate (only *Tsc2*), while the *Shank3* KO mice had elevated TRN firing and bursting. The TRN has been hypothesized to be implicated in the pathogenesis of neurodevelopmental disorders including ASD and ADHD (Krol et al., 2018). However, only limited data exists where this theory was put to test. One study found that TRN impairment underlies the ADHD-like attentional deficits in *Ptchd1* hemizygous KO mice (Wells et al., 2016). Another study found that the inhibition of a subset of TRN neurons is sufficient to produce impairments in prepulse inhibition, a marker of sensorimotor gating that is characteristically impaired in individuals with ASD (Frankland et al., 2004; Perry et al., 2007). The present study is the first to characterize TRN dysfunction in the *Tsc2* KO, and *Shank3* KO mouse lines (and a trend in the *Fmr1* KO mice), three monogenic forms of ASD; further supporting the theory of TRN dysfunction in the pathogenesis of ASD and neurodevelopmental disorders.

4.3 *Effects of UCM924:*

The last aim of the present work was to assess the effects of UCM924, a novel selective MT2 partial agonist, in these mouse models of ASD. Firstly, in the *Fmr1* mice, a trend was found in the genotype X treatment interaction in the analysis of the sociability index of the Three Chambers Test, ($p=0.058$). Since this did not reach significance, the analysis was stopped here, however it is relevant to note that if post hoc tests were performed on these data, an effect of UCM924 would

have been revealed in the KO mice such that KO mice treated with UCM924 had a higher sociability index than vehicle-treated KO mice.

UCM924 increased the social interaction time of *Tsc2* mice (main effect of treatment) and showed a trend in increasing the social novelty index of *Shank3* KO mice (p=0.059). In the present study, we did not explore the mechanism of action of UCM924's prosocial effects, but it is important to note that melatonin supplementation is not known to enhance social behaviour in individuals with ASD. Thus, future studies are warranted to better understand why the specific agonism of MT2 but not of MT2 and MT1 is capable to produce prosocial effects.

Next, UCM924 produced anxiolytic effects in several instances for the *Tsc2* cohort of mice. For example, there was a trend towards increased open arm time in the EPMT for *Tsc2* mice (p=0.052). Also, UCM924 significantly increased the distance travelled in the EPMT for these mice. The anxiolytic effects of MT2-selective agonism have been previously demonstrated (Ochoa-Sanchez et al., 2012). Although this latter study was performed in rats while the present study was performed in mice, the same general trends are present, such as that MT2 agonism can increase the time spent on the open arm of the EPMT.

Our results raise several questions. For instance, UCM924 did not produce the same effects in all the cohorts of mice. Although it is likely that UCM924 interacts differently with each KO strain due to their vastly different pathophysiologies, it was anticipated that the same general trends of the effects of UCM924 treatment would be found among all groups of mice. It is interesting to note that only the *Tsc2* mice were bred from heterozygous breeders, and only this strain had WT and KO mice housed together as littermates (the *Fmr1* and *Shank3* mice were bred from homozygous breeders and housed with littermates of the same genotype: WT or KO, not both).

This is somewhat analogous to our findings, in which we find that UCM924 only produced behavioural effects in the *Tsc2* mice (albeit a trend was observed in the TCT of the *Fmr1* mice). One potential way this may affect the behavioural results is that mice that are housed with only WT or only KO littermates might be under the presence of a cage effect. For example, if a phenotype of excessive grooming between littermates is found in the KO but not the WT mice, then this new variable would be introduced between the groups and may interact with the effect of UCM924, potentially resulting in a loss of power to detect a main effect of treatment. In fact, *Shank3* KO mice do exhibit increased repetitive grooming (Jaramillo et al., 2017; Jaramillo et al., 2020; Tatavarty et al., 2020). Although this doesn't explain this peculiar finding, it can permit future researchers to consider the breeders and housing of their mice as potential caveats in their investigations.

Lastly, UCM924 administration increased the firing and burst rate of TRN neurons of the *Fmr1* KO and *Tsc2* KO mice, normalizing their reduced spontaneous firing, and it decreased the firing rate of the TRN of *Shank3* KO mice, correcting their hyperactivation. Similar to the behavioural results, understanding the biological underpinnings of these different responses to UCM924 is beyond the scope of the present research. However, it is interesting to note that after UCM924 administration, the firing rate of TRN neurons (mean ± SEM) in *Fmr1* KO, *Tsc2* KO and *Shank3* KO mice were 7.47 ± 0.83, 6.87 ± 0.67, and 6.11 ± 0.40, respectively. Given the proximity of these means, perhaps UCM924 administration brings the firing rate of TRN neurons to some steady state of activity, irrespective of the initial firing rate, although more experiments are needed to assess this hypothesis.

One important limitation of the present study was the lack of power in many of the experiments performed (see Tables in Appendix for a complete power analysis of all the behavioural data). For

instance, while a main effect of treatment was found in the DSI for the *Tsc2* mice, it did not produce a significant prosocial effect in either the *Fmr1* or the *Shank3* mice. Importantly, the power of the treatment effect for the *Fmr1* and *Shank3* mice was 16.4% and 8.24%, respectively. Thus, our failure to reject the null hypothesis may be a result of insufficient power to detect an effect, and not necessarily that UCM924 only produces a prosocial effect in the *Tsc2* mice.

4.4 Conclusion and summary:

The objectives of the present work were to assess the behavioural phenotypes and electrophysiological properties of the TRN in three models of ASD: the *Fmr1* KO, *Tsc2* KO, and *Shank3* KO mouse lines; and to characterize the behavioural and electrophysiological effects of UCM924, a MT2 receptor selective partial agonist. To meet these objectives, we performed a variety of behavioural assays to assess social behaviour, anxiety-like behaviour, and locomotion: the Direct Social Interaction Test, Three Chambers Test, Elevated Plus-Maze Test, Light-Dark Box Test, and Open Field Test. To assess the electrophysiological properties of the TRN, single-unit recordings were taken *in vivo*, with and without microiontophoretic manipulations. The *Fmr1* KO mice display reduced social behaviour, a trend towards reduced anxiety-related behaviour and had a trend of reduced TRN activity. The *Tsc2* KO mice did not exhibit any behavioural phenotypes, but similar to the *Fmr1* mice, had significantly reduced TRN activity. The *Shank3* KO mice were hyperactive and demonstrated elevated TRN activity. The administration of UCM924 increased social behaviour and reduced anxiety-like behaviour in the *Tsc2* mice. Additionally, UCM924 increased TRN firing in the *Fmr1* and *Tsc2* KO mice, while decreasing it in the *Shank3* KO mice.

Altogether, the present work contributes to original knowledge in various ways. First, by testing and describing the behavioural phenotypes of these three mouse strains, it adds more data in the literature to be used as an assessment of the validity and translational potential of these preclinical models of ASD. Furthermore, by characterizing a novel electrophysiological dysfunction in the same brain region in three monogenic forms of ASD, our research complements existing hypotheses about the potential pathogenic role of the TRN and its potential as a therapeutic target in ASD. Lastly, we characterized the behavioural and electrophysiological effects of UCM924, a novel MT2 selective partial agonist, in three mouse models of ASD. This data, even if preliminary, will help progress the understanding of the functional role of the MT2 receptor in TRN function and its potential involvement in ASD.

REFERENCE LIST

Arons, M. H., Thynne, C. J., Grabrucker, A. M., Li, D., Schoen, M., Cheyne, J. E., . . . Garner, C. C. (2012). Autism-associated mutations in ProSAP2/Shank3 impair synaptic transmission and neurexin-neuroligin-mediated transsynaptic signaling. *J Neurosci, 32*(43), 14966-14978. doi:10.1523/JNEUROSCI.2215-12.2012

Association, A. P. (2013). Diagnostic and statistical manual of mental disorders (DSM-5®). In: American Psychiatric Pub.

Astori, S., Wimmer, R. D., Prosser, H. M., Corti, C., Corsi, M., Liaudet, N., . . . Luthi, A. (2011). The Ca(V)3.3 calcium channel is the major sleep spindle pacemaker in thalamus. *Proc Natl Acad Sci U S A, 108*(33), 13823-13828. doi:10.1073/pnas.1105115108

Bailey, D. B., Jr., Raspa, M., Olmsted, M., & Holiday, D. B. (2008). Co-occurring conditions associated with FMR1 gene variations: findings from a national parent survey. *Am J Med Genet A, 146A*(16), 2060-2069. doi:10.1002/ajmg.a.32439

Bear, M. F., Huber, K. M., & Warren, S. T. (2004). The mGluR theory of fragile X mental retardation. *Trends Neurosci, 27*(7), 370-377. doi:10.1016/j.tins.2004.04.009

Beherec, L., Lambrey, S., Quilici, G., Rosier, A., Falissard, B., & Guillin, O. (2011). Retrospective review of clozapine in the treatment of patients with autism spectrum disorder and severe disruptive behaviors. *J Clin Psychopharmacol, 31*(3), 341-344. doi:10.1097/JCP.0b013e318218f4a1

Billeiter, K. B., & Froiland, J. M. (2022). Diversity of Intelligence is the Norm Within the Autism Spectrum: Full Scale Intelligence Scores Among Children with ASD. *Child Psychiatry Hum Dev*. doi:10.1007/s10578-021-01300-9

Bozdagi, O., Sakurai, T., Papapetrou, D., Wang, X., Dickstein, D. L., Takahashi, N., . . . Buxbaum, J. D. (2010). Haploinsufficiency of the autism-associated Shank3 gene leads to deficits in synaptic function, social interaction, and social communication. *Mol Autism, 1*(1), 15. doi:10.1186/2040-2392-1-15

Capal, J. K., Williams, M. E., Pearson, D. A., Kissinger, R., Horn, P. S., Murray, D., . . . Group, T. S. (2021). Profile of Autism Spectrum Disorder in Tuberous Sclerosis Complex: Results from a Longitudinal, Prospective, Multisite Study. *Ann Neurol, 90*(6), 874-886. doi:10.1002/ana.26249

Cecon, E., Oishi, A., & Jockers, R. (2018). Melatonin receptors: molecular pharmacology and signalling in the context of system bias. *Br J Pharmacol, 175*(16), 3263-3280. doi:10.1111/bph.13950

Chevere-Torres, I., Maki, J. M., Santini, E., & Klann, E. (2012). Impaired social interactions and motor learning skills in tuberous sclerosis complex model mice expressing a dominant/negative form of tuberin. *Neurobiol Dis, 45*(1), 156-164. doi:10.1016/j.nbd.2011.07.018

Chiarotti, F., & Venerosi, A. (2020). Epidemiology of Autism Spectrum Disorders: A Review of Worldwide Prevalence Estimates Since 2014. *Brain Sci, 10*(5). doi:10.3390/brainsci10050274

Curatolo, P., & Moavero, R. (2012). mTOR Inhibitors in Tuberous Sclerosis Complex. *Curr Neuropharmacol, 10*(4), 404-415. doi:10.2174/157015912804143595

Darnell, J. C., Van Driesche, S. J., Zhang, C., Hung, K. Y., Mele, A., Fraser, C. E., . . . Darnell, R. B. (2011). FMRP stalls ribosomal translocation on mRNAs linked to synaptic function and autism. *Cell, 146*(2), 247-261. doi:10.1016/j.cell.2011.06.013

De Gregorio, D., Popic, J., Enns, J. P., Inserra, A., Skalecka, A., Markopoulos, A., . . . Gobbi, G. (2021). Lysergic acid diethylamide (LSD) promotes social behavior through mTORC1 in the excitatory neurotransmission. *Proc Natl Acad Sci U S A, 118*(5). doi:10.1073/pnas.2020705118

Devnani, P. A., & Hegde, A. U. (2015). Autism and sleep disorders. *J Pediatr Neurosci, 10*(4), 304-307. doi:10.4103/1817-1745.174438

Domich, L., Oakson, G., & Steriade, M. (1986). Thalamic burst patterns in the naturally sleeping cat: a comparison between cortically projecting and reticularis neurones. *J Physiol, 379*, 429-449. doi:10.1113/jphysiol.1986.sp016262

Drapeau, E., Dorr, N. P., Elder, G. A., & Buxbaum, J. D. (2014). Absence of strong strain effects in behavioral analyses of Shank3-deficient mice. *Dis Model Mech, 7*(6), 667-681. doi:10.1242/dmm.013821

Ehninger, D., Han, S., Shilyansky, C., Zhou, Y., Li, W., Kwiatkowski, D. J., . . . Silva, A. J. (2008). Reversal of learning deficits in a Tsc2+/- mouse model of tuberous sclerosis. *Nat Med, 14*(8), 843-848. doi:10.1038/nm1788

Ehninger, D., & Silva, A. J. (2011). Increased levels of anxiety-related behaviors in a Tsc2 dominant negative transgenic mouse model of tuberous sclerosis. *Behav Genet, 41*(3), 357-363. doi:10.1007/s10519-010-9398-1

Farmer, C. A., Chilakamarri, P., Thurm, A. E., Swedo, S. E., Holmes, G. L., & Buckley, A. W. (2018). Spindle activity in young children with autism, developmental delay, or typical development. *Neurology, 91*(2), e112-e122. doi:10.1212/WNL.0000000000005759

Fmr1 knockout mice: a model to study fragile X mental retardation. The Dutch-Belgian Fragile X Consortium. (1994). *Cell, 78*(1), 23-33. Retrieved from https://www.ncbi.nlm.nih.gov/pubmed/8033209

Frankland, P. W., Wang, Y., Rosner, B., Shimizu, T., Balleine, B. W., Dykens, E. M., . . . Silva, A. J. (2004). Sensorimotor gating abnormalities in young males with fragile X syndrome and Fmr1-knockout mice. *Mol Psychiatry, 9*(4), 417-425. doi:10.1038/sj.mp.4001432

Gantois, I., Khoutorsky, A., Popic, J., Aguilar-Valles, A., Freemantle, E., Cao, R., . . . Sonenberg, N. (2017). Metformin ameliorates core deficits in a mouse model of fragile X syndrome. *Nat Med, 23*(6), 674-677. doi:10.1038/nm.4335

Garstang, J., & Wallis, M. (2006). Randomized controlled trial of melatonin for children with autistic spectrum disorders and sleep problems. *Child Care Health Dev, 32*(5), 585-589. doi:10.1111/j.1365-2214.2006.00616.x

Gencer, O., Emiroglu, F. N., Miral, S., Baykara, B., Baykara, A., & Dirik, E. (2008). Comparison of long-term efficacy and safety of risperidone and haloperidol in children and adolescents with autistic disorder. An open label maintenance study. *Eur Child Adolesc Psychiatry, 17*(4), 217-225. doi:10.1007/s00787-007-0656-6

Goto, M., Oshima, I., Tomita, T., & Ebihara, S. (1989). Melatonin content of the pineal gland in different mouse strains. *J Pineal Res, 7*(2), 195-204. doi:10.1111/j.1600-079x.1989.tb00667.x

Hagerman, R., Au, J., & Hagerman, P. (2011). FMR1 premutation and full mutation molecular mechanisms related to autism. *J Neurodev Disord, 3*(3), 211-224. doi:10.1007/s11689-011-9084-5

Hagerman, R. J., Berry-Kravis, E., Hazlett, H. C., Bailey, D. B., Jr., Moine, H., Kooy, R. F., . . . Hagerman, P. J. (2017). Fragile X syndrome. *Nat Rev Dis Primers, 3*, 17065. doi:10.1038/nrdp.2017.65

Hebert, B., Pietropaolo, S., Meme, S., Laudier, B., Laugeray, A., Doisne, N., . . . Briault, S. (2014). Rescue of fragile X syndrome phenotypes in Fmr1 KO mice by a BKCa channel opener molecule. *Orphanet J Rare Dis, 9*, 124. doi:10.1186/s13023-014-0124-6

Huang, G., Chen, S., Chen, X., Zheng, J., Xu, Z., Doostparast Torshizi, A., . . . Shi, L. (2019). Uncovering the Functional Link Between SHANK3 Deletions and Deficiency in Neurodevelopment Using iPSC-Derived Human Neurons. *Front Neuroanat, 13*, 23. doi:10.3389/fnana.2019.00023

Huber, K. M., Gallagher, S. M., Warren, S. T., & Bear, M. F. (2002). Altered synaptic plasticity in a mouse model of fragile X mental retardation. *Proc Natl Acad Sci U S A, 99*(11), 7746-7750. doi:10.1073/pnas.122205699

Inserra, A., De Gregorio, D., Rezai, T., Lopez-Canul, M. G., Comai, S., & Gobbi, G. (2021). Lysergic acid diethylamide differentially modulates the reticular thalamus, mediodorsal thalamus, and infralimbic prefrontal cortex: An in vivo electrophysiology study in male mice. *J Psychopharmacol, 35*(4), 469-482. doi:10.1177/0269881121991569

Jaramillo, T. C., Speed, H. E., Xuan, Z., Reimers, J. M., Escamilla, C. O., Weaver, T. P., . . . Powell, C. M. (2017). Novel Shank3 mutant exhibits behaviors with face validity for autism and altered striatal and hippocampal function. *Autism Res, 10*(1), 42-65. doi:10.1002/aur.1664

Jaramillo, T. C., Xuan, Z., Reimers, J. M., Escamilla, C. O., Liu, S., & Powell, C. M. (2020). Early Restoration of Shank3 Expression in Shank3 Knock-Out Mice Prevents Core ASD-Like Behavioral Phenotypes. *eNeuro, 7*(3). doi:10.1523/ENEURO.0332-19.2020

Jockers, R., Delagrange, P., Dubocovich, M. L., Markus, R. P., Renault, N., Tosini, G., . . . Zlotos, D. P. (2016). Update on melatonin receptors: IUPHAR Review 20. *Br J Pharmacol, 173*(18), 2702-2725. doi:10.1111/bph.13536

Kamal, M., Gbahou, F., Guillaume, J. L., Daulat, A. M., Benleulmi-Chaachoua, A., Luka, M., . . . Jockers, R. (2015). Convergence of melatonin and serotonin (5-HT) signaling at MT2/5-HT2C receptor heteromers. *J Biol Chem, 290*(18), 11537-11546. doi:10.1074/jbc.M114.559542

Kazdoba, T. M., Leach, P. T., Silverman, J. L., & Crawley, J. N. (2014). Modeling fragile X syndrome in the Fmr1 knockout mouse. *Intractable Rare Dis Res, 3*(4), 118-133. doi:10.5582/irdr.2014.01024

Kazdoba, T. M., Leach, P. T., Yang, M., Silverman, J. L., Solomon, M., & Crawley, J. N. (2016). Translational Mouse Models of Autism: Advancing Toward Pharmacological Therapeutics. *Curr Top Behav Neurosci, 28*, 1-52. doi:10.1007/7854_2015_5003

Krol, A., Wimmer, R. D., Halassa, M. M., & Feng, G. (2018). Thalamic Reticular Dysfunction as a Circuit Endophenotype in Neurodevelopmental Disorders. *Neuron, 98*(2), 282-295. doi:10.1016/j.neuron.2018.03.021

Lacoste, B., Angeloni, D., Dominguez-Lopez, S., Calderoni, S., Mauro, A., Fraschini, F., . . . Gobbi, G. (2015). Anatomical and cellular localization of melatonin MT1 and MT2 receptors in the adult rat brain. *J Pineal Res, 58*(4), 397-417. doi:10.1111/jpi.12224

LeClerc, S., & Easley, D. (2015). Pharmacological therapies for autism spectrum disorder: a review. *P T, 40*(6), 389-397. Retrieved from https://www.ncbi.nlm.nih.gov/pubmed/26045648

Li, Y., Corradetti, M. N., Inoki, K., & Guan, K. L. (2004). TSC2: filling the GAP in the mTOR signaling pathway. *Trends Biochem Sci, 29*(1), 32-38. doi:10.1016/j.tibs.2003.11.007

Li, Y., Lopez-Huerta, V. G., Adiconis, X., Levandowski, K., Choi, S., Simmons, S. K., . . . Feng, G. (2020). Distinct subnetworks of the thalamic reticular nucleus. *Nature, 583*(7818), 819-824. doi:10.1038/s41586-020-2504-5

Liu, J., Clough, S. J., & Dubocovich, M. L. (2017). Role of the MT1 and MT2 melatonin receptors in mediating depressive- and anxiety-like behaviors in C3H/HeN mice. *Genes Brain Behav, 16*(5), 546-553. doi:10.1111/gbb.12369

Marco, E. J., Hinkley, L. B., Hill, S. S., & Nagarajan, S. S. (2011). Sensory processing in autism: a review of neurophysiologic findings. *Pediatr Res, 69*(5 Pt 2), 48R-54R. doi:10.1203/PDR.0b013e3182130c54

Martin, C. B., Martin, V. S., Trigo, J. M., Chevarin, C., Maldonado, R., Fink, L. H., . . . Mongeau, R. (2014). 5-HT2C receptor desensitization moderates anxiety in 5-HTT deficient mice: from behavioral to cellular evidence. *Int J Neuropsychopharmacol, 18*(3). doi:10.1093/ijnp/pyu056

Masi, A., DeMayo, M. M., Glozier, N., & Guastella, A. J. (2017). An Overview of Autism Spectrum Disorder, Heterogeneity and Treatment Options. *Neurosci Bull, 33*(2), 183-193. doi:10.1007/s12264-017-0100-y

McNaughton, C. H., Moon, J., Strawderman, M. S., Maclean, K. N., Evans, J., & Strupp, B. J. (2008). Evidence for social anxiety and impaired social cognition in a mouse model of fragile X syndrome. *Behav Neurosci, 122*(2), 293-300. doi:10.1037/0735-7044.122.2.293

Melke, J., Goubran Botros, H., Chaste, P., Betancur, C., Nygren, G., Anckarsater, H., . . . Bourgeron, T. (2008). Abnormal melatonin synthesis in autism spectrum disorders. *Mol Psychiatry, 13*(1), 90-98. doi:10.1038/sj.mp.4002016

Merikanto, I., Kuula, L., Makkonen, T., Salmela, L., Raikkonen, K., & Pesonen, A. K. (2019). Autistic Traits Are Associated With Decreased Activity of Fast Sleep Spindles During Adolescence. *J Clin Sleep Med, 15*(3), 401-407. doi:10.5664/jcsm.7662

Miral, S., Gencer, O., Inal-Emiroglu, F. N., Baykara, B., Baykara, A., & Dirik, E. (2008). Risperidone versus haloperidol in children and adolescents with AD : a randomized, controlled, double-blind trial. *Eur Child Adolesc Psychiatry, 17*(1), 1-8. doi:10.1007/s00787-007-0620-5

Moessner, R., Marshall, C. R., Sutcliffe, J. S., Skaug, J., Pinto, D., Vincent, J., . . . Scherer, S. W. (2007). Contribution of SHANK3 mutations to autism spectrum disorder. *Am J Hum Genet, 81*(6), 1289-1297. doi:10.1086/522590

Napoli, I., Mercaldo, V., Boyl, P. P., Eleuteri, B., Zalfa, F., De Rubeis, S., . . . Bagni, C. (2008). The fragile X syndrome protein represses activity-dependent translation through CYFIP1, a new 4E-BP. *Cell, 134*(6), 1042-1054. doi:10.1016/j.cell.2008.07.031

Ng, K. Y., Leong, M. K., Liang, H., & Paxinos, G. (2017). Melatonin receptors: distribution in mammalian brain and their respective putative functions. *Brain Struct Funct, 222*(7), 2921-2939. doi:10.1007/s00429-017-1439-6

Nolan, S. O., Reynolds, C. D., Smith, G. D., Holley, A. J., Escobar, B., Chandler, M. A., . . . Lugo, J. N. (2017). Deletion of Fmr1 results in sex-specific changes in behavior. *Brain Behav, 7*(10), e00800. doi:10.1002/brb3.800

Noor, A., Whibley, A., Marshall, C. R., Gianakopoulos, P. J., Piton, A., Carson, A. R., . . . Vincent, J. B. (2010). Disruption at the PTCHD1 Locus on Xp22.11 in Autism spectrum disorder and intellectual disability. *Sci Transl Med, 2*(49), 49ra68. doi:10.1126/scitranslmed.3001267

Ochoa-Sanchez, R., Comai, S., Lacoste, B., Bambico, F. R., Dominguez-Lopez, S., Spadoni, G., . . . Gobbi, G. (2011). Promotion of non-rapid eye movement sleep and activation of reticular thalamic neurons by a novel MT2 melatonin receptor ligand. *J Neurosci, 31*(50), 18439-18452. doi:10.1523/JNEUROSCI.2676-11.2011

Ochoa-Sanchez, R., Rainer, Q., Comai, S., Spadoni, G., Bedini, A., Rivara, S., . . . Gobbi, G. (2012). Anxiolytic effects of the melatonin MT(2) receptor partial agonist UCM765: comparison with melatonin and diazepam. *Prog Neuropsychopharmacol Biol Psychiatry, 39*(2), 318-325. doi:10.1016/j.pnpbp.2012.07.003

Orlova, K. A., & Crino, P. B. (2010). The tuberous sclerosis complex. *Ann N Y Acad Sci, 1184*, 87-105. doi:10.1111/j.1749-6632.2009.05117.x

Pagan, C., Delorme, R., Callebert, J., Goubran-Botros, H., Amsellem, F., Drouot, X., . . . Launay, J. M. (2014). The serotonin-N-acetylserotonin-melatonin pathway as a biomarker for autism spectrum disorders. *Transl Psychiatry, 4*, e479. doi:10.1038/tp.2014.120

Peca, J., Feliciano, C., Ting, J. T., Wang, W., Wells, M. F., Venkatraman, T. N., . . . Feng, G. (2011). Shank3 mutant mice display autistic-like behaviours and striatal dysfunction. *Nature, 472*(7344), 437-442. doi:10.1038/nature09965

Pellegrini, C., Lecci, S., Luthi, A., & Astori, S. (2016). Suppression of Sleep Spindle Rhythmogenesis in Mice with Deletion of CaV3.2 and CaV3.3 T-type Ca(2+) Channels. *Sleep, 39*(4), 875-885. doi:10.5665/sleep.5646

Perry, W., Minassian, A., Lopez, B., Maron, L., & Lincoln, A. (2007). Sensorimotor gating deficits in adults with autism. *Biol Psychiatry, 61*(4), 482-486. doi:10.1016/j.biopsych.2005.09.025

Petrasek, T., Vojtechova, I., Klovrza, O., Tuckova, K., Vejmola, C., Rak, J., . . . Waltereit, R. (2021). mTOR inhibitor improves autistic-like behaviors related to Tsc2 haploinsufficiency but not following developmental status epilepticus. *J Neurodev Disord, 13*(1), 14. doi:10.1186/s11689-021-09357-2

Pinault, D. (2004). The thalamic reticular nucleus: structure, function and concept. *Brain Res Brain Res Rev, 46*(1), 1-31. doi:10.1016/j.brainresrev.2004.04.008

Remington, G., Sloman, L., Konstantareas, M., Parker, K., & Gow, R. (2001). Clomipramine versus haloperidol in the treatment of autistic disorder: a double-blind, placebo-controlled, crossover study. *J Clin Psychopharmacol, 21*(4), 440-444. doi:10.1097/00004714-200108000-00012

Rossignol, D. A., & Frye, R. E. (2011). Melatonin in autism spectrum disorders: a systematic review and meta-analysis. *Dev Med Child Neurol, 53*(9), 783-792. doi:10.1111/j.1469-8749.2011.03980.x

Sare, R. M., Harkless, L., Levine, M., Torossian, A., Sheeler, C. A., & Smith, C. B. (2017). Deficient Sleep in Mouse Models of Fragile X Syndrome. *Front Mol Neurosci, 10*, 280. doi:10.3389/fnmol.2017.00280

Sare, R. M., Lemons, A., Song, A., & Smith, C. B. (2020). Sleep Duration in Mouse Models of Neurodevelopmental Disorders. *Brain Sci, 11*(1). doi:10.3390/brainsci11010031

Sare, R. M., Levine, M., & Smith, C. B. (2016). Behavioral Phenotype of Fmr1 Knock-Out Mice during Active Phase in an Altered Light/Dark Cycle. *eNeuro, 3*(2). doi:10.1523/ENEURO.0035-16.2016

Sato, A., Kasai, S., Kobayashi, T., Takamatsu, Y., Hino, O., Ikeda, K., & Mizuguchi, M. (2012). Rapamycin reverses impaired social interaction in mouse models of tuberous sclerosis complex. *Nat Commun, 3*, 1292. doi:10.1038/ncomms2295

Sharma, A., Hoeffer, C. A., Takayasu, Y., Miyawaki, T., McBride, S. M., Klann, E., & Zukin, R. S. (2010). Dysregulation of mTOR signaling in fragile X syndrome. *J Neurosci, 30*(2), 694-702. doi:10.1523/JNEUROSCI.3696-09.2010

Shenoy, M. D., Indla, V., & Reddy, H. (2017). Comprehensive Management of Autism: Current Evidence. *Indian J Psychol Med, 39*(6), 727-731. doi:10.4103/IJPSYM.IJPSYM_272_17

Spencer, C. M., Alekseyenko, O., Hamilton, S. M., Thomas, A. M., Serysheva, E., Yuva-Paylor, L. A., & Paylor, R. (2011). Modifying behavioral phenotypes in Fmr1KO mice: genetic background differences reveal autistic-like responses. *Autism Res, 4*(1), 40-56. doi:10.1002/aur.168

Sureda, B., Alberca, R., & Navarro, E. (1991). [Pituitary study in benign intracranial hypertension]. *Arch Neurobiol (Madr), 54*(4), 151-155. Retrieved from https://www.ncbi.nlm.nih.gov/pubmed/1958126

Tatavarty, V., Torrado Pacheco, A., Groves Kuhnle, C., Lin, H., Koundinya, P., Miska, N. J., . . . Turrigiano, G. G. (2020). Autism-Associated Shank3 Is Essential for Homeostatic Compensation in Rodent V1. *Neuron, 106*(5), 769-777 e764. doi:10.1016/j.neuron.2020.02.033

Thankachan, S., Katsuki, F., McKenna, J. T., Yang, C., Shukla, C., Deisseroth, K., . . . Basheer, R. (2019). Thalamic Reticular Nucleus Parvalbumin Neurons Regulate Sleep Spindles and Electrophysiological Aspects of Schizophrenia in Mice. *Sci Rep, 9*(1), 3607. doi:10.1038/s41598-019-40398-9

Thomson, D. M., Mitchell, E. J., Openshaw, R. L., Pratt, J. A., & Morris, B. J. (2021). Mice lacking melatonin MT2 receptors exhibit attentional deficits, anxiety and enhanced social interaction. *J Psychopharmacol, 35*(10), 1265-1276. doi:10.1177/02698811211032439

Tordjman, S., Anderson, G. M., Bellissant, E., Botbol, M., Charbuy, H., Camus, F., . . . Touitou, Y. (2012). Day and nighttime excretion of 6-sulphatoxymelatonin in adolescents and young adults with autistic disorder. *Psychoneuroendocrinology, 37*(12), 1990-1997. doi:10.1016/j.psyneuen.2012.04.013

Uchino, S., & Waga, C. (2013). SHANK3 as an autism spectrum disorder-associated gene. *Brain Dev, 35*(2), 106-110. doi:10.1016/j.braindev.2012.05.013

Vantomme, G., Osorio-Forero, A., Luthi, A., & Fernandez, L. M. J. (2019). Regulation of Local Sleep by the Thalamic Reticular Nucleus. *Front Neurosci, 13*, 576. doi:10.3389/fnins.2019.00576

Verkerk, A. J., Pieretti, M., Sutcliffe, J. S., Fu, Y. H., Kuhl, D. P., Pizzuti, A., . . . et al. (1991). Identification of a gene (FMR-1) containing a CGG repeat coincident with a breakpoint cluster region exhibiting length variation in fragile X syndrome. *Cell, 65*(5), 905-914. doi:10.1016/0092-8674(91)90397-h

Waltereit, R., Japs, B., Schneider, M., de Vries, P. J., & Bartsch, D. (2011). Epilepsy and Tsc2 haploinsufficiency lead to autistic-like social deficit behaviors in rats. *Behav Genet, 41*(3), 364-372. doi:10.1007/s10519-010-9399-0

Wan, Q., Man, H. Y., Liu, F., Braunton, J., Niznik, H. B., Pang, S. F., . . . Wang, Y. T. (1999). Differential modulation of GABAA receptor function by Mel1a and Mel1b receptors. *Nat Neurosci, 2*(5), 401-403. doi:10.1038/8062

Wells, M. F., Wimmer, R. D., Schmitt, L. I., Feng, G., & Halassa, M. M. (2016). Thalamic reticular impairment underlies attention deficit in Ptchd1(Y/-) mice. *Nature, 532*(7597), 58-63. doi:10.1038/nature17427

You, Q. L., Luo, Z. C., Luo, Z. Y., Kong, Y., Li, Z. L., Yang, J. M., . . . Gao, T. M. (2021). Involvement of the thalamic reticular nucleus in prepulse inhibition of acoustic startle. *Transl Psychiatry, 11*(1), 241. doi:10.1038/s41398-021-01363-1

Yu, S., Pritchard, M., Kremer, E., Lynch, M., Nancarrow, J., Baker, E., . . . et al. (1991). Fragile X genotype characterized by an unstable region of DNA. *Science, 252*(5009), 1179-1181. doi:10.1126/science.252.5009.1179

Yuan, E., Tsai, P. T., Greene-Colozzi, E., Sahin, M., Kwiatkowski, D. J., & Malinowska, I. A. (2012). Graded loss of tuberin in an allelic series of brain models of TSC correlates with survival, and biochemical, histological and behavioral features. *Hum Mol Genet, 21*(19), 4286-4300. doi:10.1093/hmg/dds262

Zaboski, B. A., & Storch, E. A. (2018). Comorbid autism spectrum disorder and anxiety disorders: a brief review. *Future Neurol, 13*(1), 31-37. doi:10.2217/fnl-2017-0030

Zalfa, F., Giorgi, M., Primerano, B., Moro, A., Di Penta, A., Reis, S., . . . Bagni, C. (2003). The fragile X syndrome protein FMRP associates with BC1 RNA and regulates the translation of specific mRNAs at synapses. *Cell, 112*(3), 317-327. doi:10.1016/s0092-8674(03)00079-5

Zikopoulos, B., & Barbas, H. (2006). Prefrontal projections to the thalamic reticular nucleus form a unique circuit for attentional mechanisms. *J Neurosci, 26*(28), 7348-7361. doi:10.1523/JNEUROSCI.5511-05.2006

APPENDIX

Power analysis of behavioral experiments:

Power analyses were computed using G*Power and SPSS software (G*Power for parametric tests and SPSS for non-parametric tests). Effect size was computed by inputting the partial eta squared ($\eta^2_{partial}$), which was calculated using the following formula: $\eta^2_{partial} = SS_{GROUP}/ (SS_{GROUP} + SS_{ERROR})$, where SS is the sum of squares. Post hoc power analyses were performed to calculate the observed power, using an alpha value of 0.05. A priori power analyses were performed to calculate the required sample size for 95% power, using alpha and beta values of 0.05.

Fmr1 mice						
Experiment	Sample size		Total n	Effect size	Observed power	n for 95% power
DSI	WT veh: 10 KO veh:12	WT UCM: 9 KO UCM: 17	48	Genotype: 0.382 Treatment: 0.144 Interaction: 0.188	Genotype: 0.734 Treatment: 0.164 Interaction: 0.246	Genotype: 92 Treatment: 629 Interaction: 372
TCT sociability	WT veh: 10 KO veh: 12	WT UCM: 8 KO UCM: 17	47	Genotype: 0.241 Treatment: 0.305 Interaction: 0.297	Genotype: 0.366 Treatment: 0.534 Interaction: 0.511	Genotype: 226 Treatment: 142 Interaction: 150
TCT social novelty	WT veh: 9 KO veh: 12	WT UCM: 8 KO UCM: 16	45	Genotype: 0.153 Treatment: 0.0947 Interaction: 0.0190	Genotype: 0.171 Treatment: 0.0952 Interaction: 0.0518	Genotype: 557 Treatment: 1451 Interaction: 35832
EPMT time in open arm	WT veh: 11 KO veh: 12	WT UCM: 9 KO UCM: 17	49	Genotype: 0.283 Treatment: 0.0650 Interaction: 0.0574	Genotype: 0.492 Treatment: 0.073 Interaction: 0.0679	Genotype: 164 Treatment: 3078 Interaction: 3942
EPMT entries to open arm	WT veh: 11 KO veh: 12	WT UCM: 9 KO UCM: 17	49	Genotype: 0.137 Treatment: 0.0268 Interaction: 0.0927	Genotype: 0.155 Treatment: 0.0539 Interaction: 0.0974	Genotype: 700 Treatment: 18130 Interaction: 1513
EPMT distance travelled	WT veh: 11 KO veh: 12	WT UCM: 9 KO UCM: 17	49	Genotype: 0.642 Treatment: 0.261 Interaction: 0.0728	Genotype: 0.993 Treatment: 0.433 Interaction: 0.0789	Genotype: 34 Treatment: 193 Interaction: 2456
OFT time in center	WT veh: 4 KO veh: 8	WT UCM: 6 KO UCM: 8	26	Genotype: 0.0103 Treatment: 0.0448 Interaction: 0.287	Genotype: 0.0503 Treatment: 0.0555 Interaction: 0.288	Genotype: 123027 Treatment: 6489 Interaction: 160
OFT entries to center	WT veh: 4 KO veh: 8	WT UCM: 6 KO UCM: 8	26	Genotype: 0.00445 Treatment: 0.170 Interaction: 0.272	Genotype: 0.0501 Treatment: 0.132 Interaction: 0.263	Genotype: 656377 Treatment: 452 Interaction: 179
OFT distance travelled	WT veh: 3 KO veh: 5	WT UCM: 3 KO UCM: 7	18	Genotype: 0.100 Treatment: 0.223 Interaction: 0.179	Genotype: 0.0682 Treatment: 0.143 Interaction: 0.109	Genotype: 1301 Treatment: 263 Interaction: 410

Tsc2 mice						
Experiment	Sample size		Total n	Effect size	Observed power	n for 95% power
DSI	WT veh: 14 KO veh: 16	WT UCM: 10 KO UCM: 10	50	Genotype:0.252 Treatment: 0.393 Interaction: 0.148	Genotype: 0.415 Treatment: 0.776 Interaction: 0.177	Genotype: 207 Treatment: 87 Interaction: 594
TCT sociability	WT veh: 9 KO veh: 11	WT UCM: 10 KO UCM: 10	40	Genotype: 0.165 Treatment: 0.0934 Interaction: 0.0260	Genotype: 0.174 Treatment: 0.0887 Interaction: 0.0529	Genotype: 479 Treatment: 1493 Interaction: 19275
TCT social novelty	WT veh: 9 KO veh: 11	WT UCM: 10 KO UCM: 10	40	Genotype: 0.122 Treatment: 0.00535 Interaction: 0.0105	Genotype: 0.117 Treatment: 0.0501 Interaction: 0.0505	Genotype: 871 Treatment: 454282 Interaction: 117703
EPMT time in open arm	WT veh: 9 KO veh: 11	WT UCM: 10 KO UCM: 10	40	Genotype: 0.124 Treatment: 0.336 Interaction: 0.125	Genotype: 0.119 Treatment: 0.542 Interaction: 0.120	Genotype: 844 Treatment: 118 Interaction: 839
EPMT entries to open arm	WT veh: 9 KO veh: 11	WT UCM: 10 KO UCM: 10	40	Genotype: 0.0422 Treatment: 0.0680 Interaction: 0.0422	Genotype: 0.0578 Treatment: 0.0703 Interaction: 0.0578	Genotype: 7315 Treatment: 2812 Interaction: 7315
EPMT distance travelled	WT veh: 9 KO veh: 11	WT UCM: 10 KO UCM: 10	40	Genotype: 0.0156 Treatment: 0.521 Interaction: 0.0206	Genotype: 0.0511 Treatment: 0.894 Interaction: 0.0518	Genotype: 53293 Treatment: 50 Interaction: 30740
OFT time in center	WT veh: 8 KO veh: 10	WT UCM: 7 KO UCM: 5	30	Genotype: 0.151 Treatment: 0.124 Interaction: 0.401	Genotype: 0.125 Treatment: 0.101 Interaction: 0.561	Genotype: 575 Treatment: 841 Interaction: 83
OFT entries to center	WT veh: 8 KO veh: 10	WT UCM: 7 KO UCM: 5	30	Genotype: 0.200 Treatment: 0.263 Interaction: 0.363	Genotype: 0.184 Treatment: 0.284 Interaction: 0.483	Genotype: 328 Treatment: 190 Interaction: 101
OFT distance travelled	WT veh: 6 KO veh: 8	WT UCM: 4 KO UCM: 3	21	Genotype: 0.0116 Treatment: 0.395 Interaction: 0.0604	Genotype: 0.0503 Treatment: 0.400 Interaction: 0.0579	Genotype: 96040 Treatment: 86 Interaction: 3570

Shank3 mice						
Experiment	Sample size		Total n	Effect size	Observed power	n for 95% power
DSI	WT veh: 11 KO veh: 13	WT UCM: 13 KO UCM: 11	48	Genotype: 0.102 Treatment: 0.0778 Interaction: 0.123	Genotype: 0.106 Treatment: 0.0824 Interaction: 0.134	Genotype: 1253 Treatment: 2149 Interaction: 844
TCT sociability	WT veh: 11 KO veh: 13	WT UCM: 13 KO UCM: 11	48	Genotype: 0.215 Treatment: 0.124 Interaction: 0.0394	Genotype: 0.301 Treatment: 0.134 Interaction: 0.0582	Genotype: 283 Treatment: 845 Interaction: 8370
TCT social novelty	WT veh: 11 KO veh: 13	WT UCM: 13 KO UCM: 11	48	Genotype: 0.221 Treatment: 0.292 Interaction: 0.159	Genotype: 0.323 Treatment: 0.508 Interaction: 0.190	Genotype: 268 Treatment: 155 Interaction: 516
EPMT time in open arm	WT veh: 11 KO veh: 13	WT UCM: 13 KO UCM: 11	48	Genotype: 0.172 Treatment: 0.138 Interaction: 0.0100	Genotype: 0.214 Treatment: 0.155 Interaction: 0.0505	Genotype: 442 Treatment: 681 Interaction: 128982
EPMT entries to open arm	WT veh: 11 KO veh: 13	WT UCM: 13 KO UCM: 11	48	Genotype: 0.119 Treatment: 0.199 Interaction: 0.154	Genotype: 0.127 Treatment: 0.272 Interaction: 0.182	Genotype: 917 Treatment: 330 Interaction: 548
EPMT distance travelled	WT veh: 11 KO veh: 13	WT UCM: 13 KO UCM: 11	48	Genotype: 0.0100 Treatment: 0.189 Interaction: 0.0775	Genotype: 0.0505 Treatment: 0.249 Interaction: 0.0822	Genotype: 128982 Treatment: 367 Interaction: 2164
OFT time in center	WT veh: 6 KO veh: 8	WT UCM: 12 KO UCM: 11	37	Genotype: 0.433 Treatment: 0.201 Interaction: 0.240	Genotype: 0.725 Treatment: 0.220 Interaction: 0.294	Genotype: 72 Treatment: 325 Interaction: 228
OFT entries to center	WT veh: 6 KO veh: 8	WT UCM: 12 KO UCM: 11	37	Genotype: 0.659 Treatment: 0.0800 Interaction: 0.177	Genotype: 0.973 Treatment: 0.076 Interaction: 0.182	Genotype: 33 Treatment: 2032 Interaction: 415
OFT distance travelled	WT veh: 4 KO veh: 3	WT UCM: 5 KO UCM: 7	19	Genotype: 0.641 Treatment: 0.0986 Interaction: 0.338	Genotype: 0.742 Treatment: 0.0688 Interaction: 0.281	Genotype: 34 Treatment: 1340 Interaction: 116

Appendix Tables: Power analysis for *Fmr1, TSC2 and Shank 3* mice behavioural experiments

Where it is not specified, the sample size indicates the number of mice tested. The present tables include the effect size, observed power (post hoc power analysis), and the required sample size for 95% power (a priori power analysis) for each ANOVA factor for each behavioural and electrophysiological experiment.